

REFERENCES

- Abthagir, P.S., Dhanalakshmi, K., and Saraswathi, R. (1998) Thermal studies on polyindole and polycarbazole. Synthetic Metals, 93(1), 1-7.
- Abthagir, P.S. and Saraswathi, R. (2004) Charge transport and thermal properties of polyindole and polycarbazole and their derivatives. Thermochimica Acta, 424(1-2), 25-35.
- Bar-Cohen, Y. (2nd ed). (2004) Electroactive Polymer (EAP) as Artificial Muscles: Reality, Potential, and Challenges, The United States of America: SPIE.
- Bar-Cohen, Y. (2002) Electro-active polymers: current capabilities and challenges. Paper presented at Proceeding of SPIE Smart Structures and Materials Symposium, 4695-4702.
- Baughman, R.H. (1996) Conducting polymer artificial muscles. Synthetic Metals, 79(3), 339-353.
- Bini, E., Knight, D.P., and Kaplan, D.L. (2004) Mapping domain structures in silks from insects and spider related to protein assembly. Journal of Molecular Biology, 335(1), 27-40.
- Carbazole. Retrieved April 16, 2012. From <http://en.wikipedia.org/wiki/Carbazole>
- Chansai, P., Sirivat, A., Niamlang, S., Chotpattananont, D., and Viravaidya-Pasuwat, K. (2009) Controlled transdermal iontophoresis of sulfosalicylic acid from polypyrrole/poly(acrylic acid) hydrogel. International Journal of Pharmaceutics, 381(1), 25-33.
- Fibroin. Retrieved April 16, 2012. From <http://en.wikipedia.org/wiki/Fibroin>.
- Freddi, G., Romano, M., Massafra, M.R., and Tsukada, M. (1995) Silk fibroin/cellulose blend films: preparation, structure, and physical properties. Journal of Applied Polymer Science, 56(12), 1537-1545.
- Frommer, J.E. (1986) Conducting polymer solution. Accounts of Chemical Research, 19(1), 2-9.
- Grath, K.M. and Kaplan, D.L. (1997) Protein based Materials, Boston: Birkhauser.
- Gupta, B., Singh, A.K., and Prakash, R. (2010) Electrolyte effects on various properties of polycarbazole. Thin Solid Films, 519(3), 1016-1019.

- Gupta, B. and Prakash, R. (2010) Interfacial polymerization of carbazole: morphology controlled synthesis. *Synthetic Metals*, 160(5-6), 523-528.
- Harun, M.H., Saion, E., Kassim, A., Yahya, N., and Mahmud, E. (2007) Conjugated conducting polymers: A brief overview. *JASA* 2, 63-68.
- Hiamtup, P., Sirivat, A., and Jamieson, A.M. (2008) Electromechanical response of a soft and flexible actuator based on polyaniline particles embedded in a cross-linked poly(dimethyl siloxane) network. *Materials Science and Engineering C*, 28, 1044-1051.
- Inselt, G. (2003) Formation and redox behavior of polycarbazole prepared by electropolymerization of solid carbazole crystals immobilized on an electrode surface. *Solid State Electrochem*, 7(8), 503-510.
- Jin, H.J., Myung, S.J., Kim, H.S., Jung, W., and Kim, J. (2006) Silkworm protein: its possibility as an actuator. Paper presented at *Proceedings of SPIE*, 6168, 616821-616826.
- Kim, U.J., Park, J., Li, C., Jin, H.K., Valluzzi, R., and Kaplan, D.L. (2004) Structure and properties of silk hydrogels. *Biomacromolecules*, 5(3), 789-792.
- Kunanurusapong, R., and Sirivat, A. (2007) Poly(p-phenylene) and acrylic elastomer blends for electroactive application. *Materials Science and Engineering A*, 454-455, 453-460.
- Kunchornsup, W. and Sirivat, A. (2012) Physically cross-linked cellulosic gel via 1-butyl-3-methylimidazolium chloride ionic liquid and its electrorheological response. *Sensors and Actuators A: Physical*, 175, 155-164.
- Li, M., Lu, S., Wu, Z., Tan, K., Minoura, N., and Kuga, S. (2002) Structure and properties of silk fibroin-poly(vinyl alcohol) gel. *Macromolecules*, 30(2), 89-94
- Lu, Q., Huang, Y., Li, M., Zuo, B., Lu, S., Wang, J., Zhu, H., and Kaplan, D.L. (2011) Silk fibroin electrogelation mechanisms. *Acta Biomaterialia*, 7(6), 2394-2400.
- Macit, H., Sen, S., and Sacak, M. (2005) Electrochemical synthesis and characterization of polycarbazole. *Journal of Applied Polymer Science*, 96(3), 894-898.

- Matsumoto, A., Chen, J., Collette, A.L., Kim, U.J., Altman, G.H., Cebe, P., and Kaplan, D.L. (2006) Mechanisms of silk fibroin sol-gel transition. Journal of Physical Chemistry, 110(43), 21630-21638.
- Mirfakhrai, T., Madden, D. W., and Baughman, R.H. (2007) Polymer artificial muscles. Materialtoday, 10(4), 30-38.
- Morin, J., Lecterc, M., Ades, D., and Siove, A. (2005) Polycarbazoles: 25 years of progress. Macromolecular Rapid Communication, 26(10), 761-778.
- Moschou, E., Peteu, S., Bachas, L.G., Madou, M.J., and Daunert, S. (2004) Artificial muscle material with fast electroactuation under natural pH condition. Chemistry of Materials, 16, 2499-2502.
- Moschou, E.A., Madou, M.J., Bachas, L.G., and Daunert, S. (2005) voltage-switchable actifical muscles actuating at near neutral pH. Sensors and Actuators B, In press.
- Niamlang, S. and Sirivat, A. (2008) Electromechanical response of a crosslonked polydimethylsiloxane. Macromolecule Symposia, 264, 176-183.
- Nogueira, G.M., de Moraes, M.A., Rodas, A.C., Higa, O.Z., and Beppu, M.M. (2011) Hydrogels from silk fibroin metastable solution: Formation and characterization from a biomaterial perspective. Materials Science and Engineering: C, 31(5), 997-1001.
- Ntavrouli, N., Kyrazis, A., and Tsitsilianis, C. (2008) Reversible hydrogels from an ampholytic An(B-b-C)n heteroarm star block terpolymer. Macromolecular Chemistry and Physics, 209, 2241-2247.
- Numata, K., Katashima, T., and Sakai, T. (2011) State of water, molecular structure, and cytotoxicity of silk hydrogels. Macromolecules, 12, 2137-2144.
- Palakodeti, R., and Kessler, M.R. (2006) Influence of frequency and prestrain on the mechanical efficiency of dielectric electroactive polymer actuators. Materials Letters, 60(29-30), 3437-3440.
- Petcharoen, K., and Sirivat, A. (2013) Electrostrictive properties of thermoplastic polyurethane elastomer: effects of urethane type and soft-hard segment composition. Current Applied Physics, (1-13), Accepted manuscript online.

- Kupfer, K. (2005) Electromagnetic Aquametry. Boston: Springer (39-70).
- Pratt, C. (1996) Conducting polymers. Retrieved April 16, 2012. From <http://www.ims.vanderbilt.edu/mse150/wittg10/cpoly.pdf>.
- Prissanaroon, W., Ruangchuay, L., Sirivat, A., and Schwank, J. (2000) Electrical conductivity response of dodecylbenzene sulfonic acid-doped polypyrrole film to SO₂-N₂ mixtures. Synthetic Metals, 114(1), 65-72.
- Raj, V., Madheswari, D., and Ali, M. M. (2010) Chemical formation, characterization and properties of polycarbazole. Journal of Applied Polymer Science, 116(1), 147-154.
- Sarmad, S., Yenici, G., Gurkan, K., Keceli, G., and Gurdag, G. (2013) Electric field responsive chitosan-poly(N,N-dimethyl acrylamide) semi-IPN gel films, and their dielectric, thermal, and swelling characterization. Smart Materials and Structures, 22 055010.
- Siove, A. and Ades, D. (2004) Synthesis by oxidative polymerization with FeCl₃ of a fully aromatic twisted poly(3,6-carbazole) with a blue-violet luminescence. Polymer, 45(12), 4049-4054.
- Sohn, S., Strey, H.H., and Gido, S.P. (2004) Phase behavior and hydration of silk fibroin. Biomacromolecules, 5(3), 751-757.
- Sengwa, R. and Kaur, K. (2000) Dielectric dispersion studies of poly(vinyl alcohol) in aqueous solutions. Polymer International, 49, 1314-1320.
- Taoudi, H., Bernede, J.C., Del Valle, M.A., Bonnet, A., Molinie, P., Morsi, M., Diaz, F., Tregovet, Y., and Bereau, A. (2000) Polycarbazole obtained by electrochemical polymerization of monomers either in solution or in thin film form. Journal of Applied Polymer Science, 75(13), 1561-1568.
- Thipdech, P., Kunanurusapong, R., and Sirivat, A. (2008) Electromechanical responses of poly(3-thiopheneacetic acid)/acrylonitrile-butadiene rubber. Express Polymer Letter, 2(12), 866-877.
- Thongsak, K., Kunanuruksapong, R., Sirivat, A., and Lerdwijitjarud, W. (2010) Electroactive styrene-isoprene-styrene triblock copolymer: effects of morphology and electric field. Material Science and Engineering A, 527, 2504-2509.

- Tong, C. and Vilgis, T.A., (2008) Enhanced orientational ordering of water dipoles in uniaxially stretched hydrogels. Journal of Physical Chemistry B, 112, 16490-16496.
- Tungkavet, T., Seetapan, N., Pattavarakorn, D, and Sirivat, A. (2012) Improvements of electromechanical properties of gelatin hydrogels by blending with nanowire polypyrrole: effects of electric field and temperature. Polymer International, 61, 825-833.
- Vepari, C. and Kaplan, D.L. (1997) Silk as biomaterial. Boston: Birkhauser.
- Verghese, M.M., Sundaresan, N.S., Basu, T., and Malhotra, B.D. (1995) Electroactivity and proton doping of polycarbazole. Journal of Materials Science Letters, 14(6), 401-404.
- Wang, X., Kluge, J.A., Leisk, G.G., and Kaplan, D.L. (2008) Sonication-induced gelation of silk fibroin for cell encapsulation. Biomaterials, 29(8), 1054-1064.
- Wichiansee, W. and Sirivat, A. (2009) Electrorhrological properties of poly(dimethylsiloxane) and poly(3,4-ethylenedioxy thiophene)/poly(styrene sulfonic acid)/ethylene glycol blends. Materials Science and Engineering C, 29(1), 78-84.
- Zhuang, D.X. and Chen, P.Y. (2009) Electrochemical formation of polycarbazole films in air- and water-stable room-temperature ionic liquids. Journal of Electroanalytical Chemistry, 626(1-2), 197-200.

APPENDICES

Appendix A Determination the Functional Group of Polycarbazole and Silk Fibroin Hydrogel by Fourier Transform Infrared Spectroscopy

Polycarbazole (PCZ) was synthesized via the oxidative polymerization of carbazole to obtain synthesized PCZ (Gupta *et al.*, 2010). The synthesized PCZ was dedoped by immersing in an ammonium hydroxide solution to neutralize PCZ, and then doped with the various mole ratios of hydrochloric acid. The mole ratio of hydrochloric acid per carbazole repeating unit ($N_{HCl}:N_{PCZ}$) were 1:1, 10:1, 100:1, 200:1, and 300:1. Optical grade KBr was used as the background material. The polymers were first characterized for the functional groups by the FTIR spectrometer (Thermo Nicolet, Nexus 670) in the transmission mode with 64 scans at a resolution of 4 cm^{-1} .

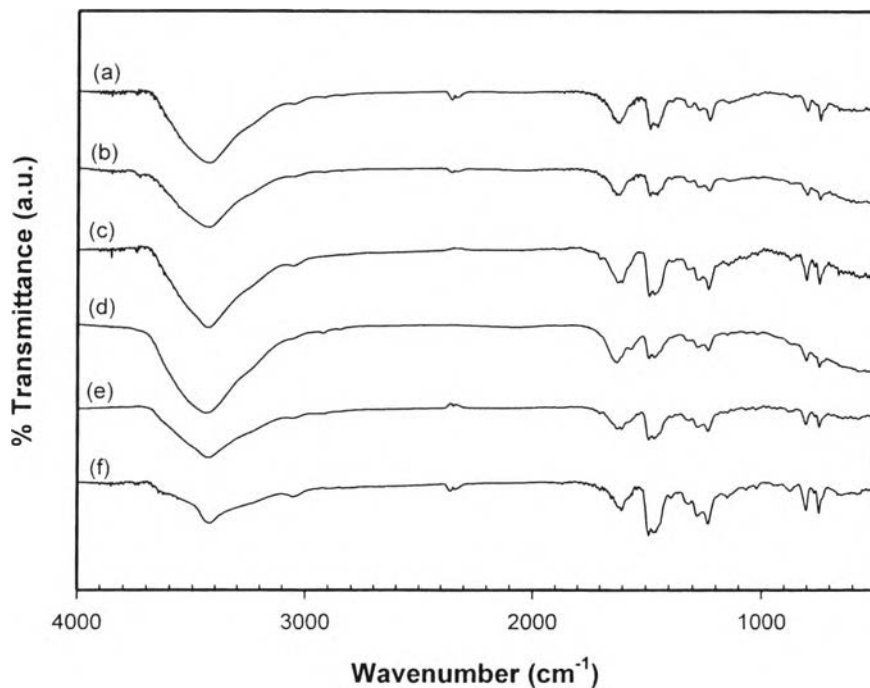


Figure A1 The FTIR spectra of: (a) dedoped PCZ; (b) doped 1:1 PCZ; (c) doped 10:1 PCZ; (d) doped 100:1 PCZ; (e) doped 200:1 PCZ; and (f) doped 300:1 PCZ.

The FTIR spectra of dedoped PCZ and doped PCZ with hydrochloric acid are shown for comparison in Figure A1. The peak at 3400 cm^{-1} refers to the N-H stretching of heteroaromatics, where the others FT-IR peaks represent the C=C stretching of the aromatic compound at $1600\text{-}1625\text{ cm}^{-1}$, the C-N stretching of substitutions at $1400\text{-}1490\text{ cm}^{-1}$, the C-H in plane bending at $1200\text{-}1235\text{ cm}^{-1}$, the C-H deformation of trisubstituted benzene ring at $800\text{-}875\text{ cm}^{-1}$, the C-H out-of-plane bending at $700\text{-}750\text{ cm}^{-1}$ (Gupta *et al.*, 2010, Raj *et al.*, 2010). With increasing amount of dopant beyond $\text{N}_{\text{HCl}}:\text{N}_{\text{PCZ}}$ to 100:1, the peak intensity of the N-H stretching is reduced.

Table A1 The FTIR assignments of polycarbazole

Wavenumber (cm^{-1})	Assignment Peaks	References
3300-3400	N-H stretching	Raj <i>et al.</i> , 2010
1600-1625	C=C stretching	Gupta <i>et al.</i> , 2010
1400-1490	C-N stretching	Raj <i>et al.</i> , 2010
1200-1235	C-H in plane bending	Raj <i>et al.</i> , 2010
800-875	C-H stretching	Gupta <i>et al.</i> , 2010
700-750	C-H out-of-plane bending	Raj <i>et al.</i> , 2010

For the pure silk fibroin (SF) and crosslinked SF hydrogel, samples were freeze-dried before grinding with optical grade KBr, compressed into pellets, and characterized with the FTIR spectrometer (Thermo Nicolet, Nexus 760) in the absorption mode with 64 scans at a resolution of 4 cm^{-1} .

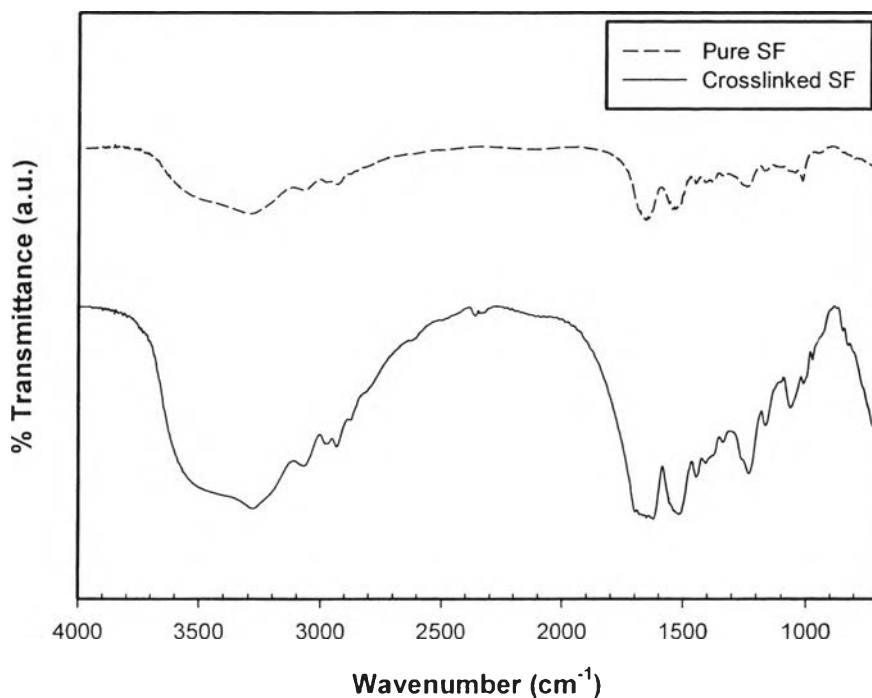


Figure A2 The FTIR spectra of pure SF and crosslinked SF.

Figure A2 shows the FTIR spectra of pure SF and crosslinked SF with glutaraldehyde (GTA). The characteristic peaks represent the N-H stretching at 3200-3300 cm⁻¹, the amide I at 1625-1700 cm⁻¹, the amide II at 1520-1550 cm⁻¹, the C-H stretching and the C-H bending at 2900 and 1450 cm⁻¹, respectively. The crosslinked SF gel samples shows an intense peak at 1240-1300 cm⁻¹ representing the amide III due to the transformation of random coils to the β -sheet structure (Kim *et al.*, 2004, Matsumoto *et al.*, 2006, Weska *et al.*, 2009, Lu *et al.*, 2011).

Table A2 The FTIR assignments of pure SF and crosslinked SF gels

Wavenumber (cm^{-1})	Assignment peaks	References
3200-3300	N-H stretching	Lu <i>et al.</i> 2011
2900-3000	C-H stretching	Matsumoto <i>et al.</i> , 2006
1625-1700	Amide I (C=O stretching)	Kim <i>et al.</i> , 2004 Weskaet <i>al.</i> ,2009
1520-1550	Amide II (N-H bending, C-H stretching)	Kim <i>et al.</i> , 2004 Weskaet <i>al.</i> ,2009
1450-1500	C-H bending	Matsumoto <i>et al.</i> , 2006
1240-1300	Amide III (C-N stretching, C=O bending)	Kim <i>et al.</i> , 2004 Weskaet <i>al.</i> ,2009

Appendix B Thermal Properties of Polycarbazole and Silk Fibroin Hydrogel

The thermal behavior of polymers was determined by the thermogravimetric analyzer (Thermo, TGA Q 50). The characterization was carried out by weighting a powder sample of 4-5 mg and placed it in a platinum pan, and then heated it under nitrogen flow with the heating rate 10°C/min from 30 to 900 °C.

There are two transition temperatures for the dedoped PCZ (De_PCZ) and the doped 100:1 PCZ. The first transition (400-600 °C) can be assigned to the elimination of dopants and the second transition (700-800 °C) can be referred to the decomposition of the polymeric chain (Abthagiret *et al.*, 2004).

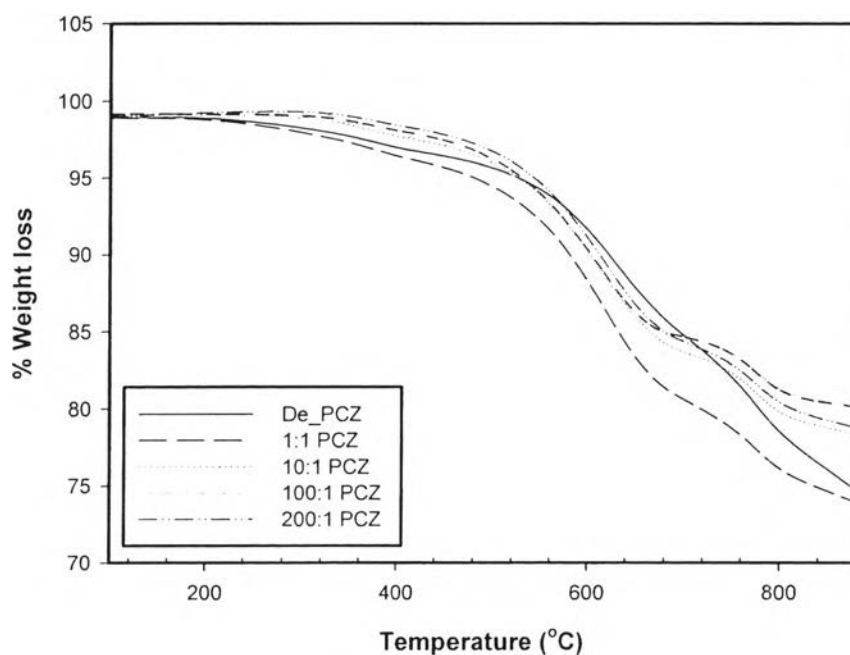


Figure B1 The TGA thermograms of De_PCZ and doped PCZ with various amount of doping levels.

Table B1 The summary of degradation temperature and percent weight loss in TGA thermograms of De_PCZ and doped PCZ at various doping levels

Sample	T _d (°C)	% Weight loss
De_PCZ	554.55	12.38
	748.46	8.88
Doped 1:1 PCZ	541.41	15.83
	748.64	5.84
Doped 10:1 PCZ	534.78	14.18
	748.45	4.94
Doped 100:1 PCZ	527.46	13.15
	750.01	4.484
Doped 200:1 PCZ	535.02	14.23
	747.55	5.00
Doped 300:1 PCZ	528.15	13.30
	744.83	4.393

There are two transitions for pure SF and crosslinked SF gels (4, 5%v/v SF solution crosslinked with 0.01, 0.05, 0.1, 0.5, and 1%v/v glutaraldehyde (GTA) respectively. The first transition (80-120 °C) refers to the loss of moisture and low temperature volatile species in the samples (Motta *et al.*, 2003). The second transition (270-500 °C) refers to the breakdown of the side chain group of amino acid residue and the silk fibroin degradation (Weska *et al.*, 2009). The TGA thermograms of the pure SF and crosslinked SF show that the decomposition temperature does not change significantly, while % weight loss slightly decreases with increasing amount of GTA as the crosslinking agent.

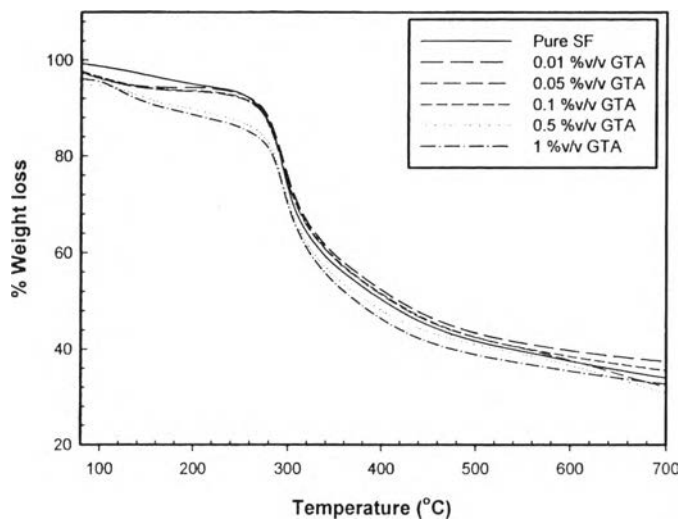


Figure B2 The TGA thermograms of pure SF and crosslinked 4%v/v SF solution with 0.01, 0.05, 0.1, 0.5, and 1%v/v of GTA.

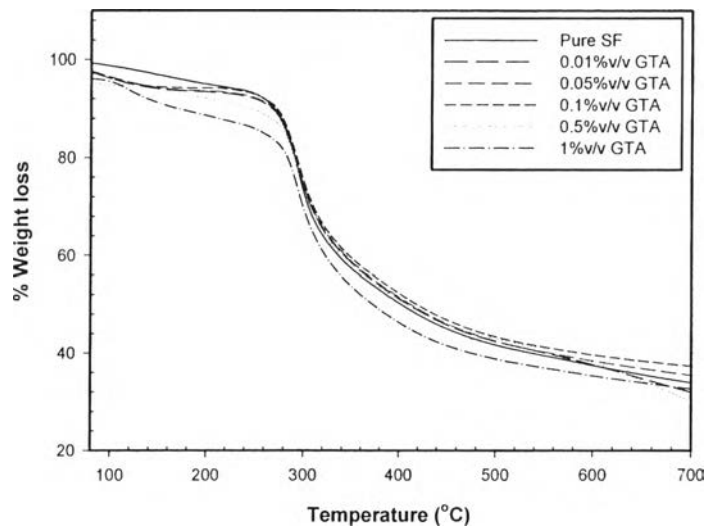


Figure B3 The TGA thermograms of pure SF and crosslinked 5%v/v SF solution with 0.01, 0.05, 0.1, 0.5, and 1%v/v of GTA.

Table B2 The summary of degradation temperature and percent weight loss in TGA thermograms of pure SF and crosslinked SF solution with various amounts of GTA

Sample	T _d (°C)	% Weight loss
Pure SF	275.69	55.07
0.01%v/v GTA in 4%v/v SF	270.39	54.89
0.05%v/v GTA in 4%v/v SF	271.60	54.80
0.1%v/v GTA in 4%v/v SF	270.82	54.00
0.5%v/v GTA in 4%v/v SF	276.71	54.00
1.0%v/v GTA in 4%v/v SF	277.79	52.86
0.01%v/v GTA in 5%v/v SF	271.34	52.88
0.05%v/v GTA in 5%v/v SF	267.83	54.95
0.1%v/v GTA in 5%v/v SF	271.56	54.88
0.5%v/v GTA in 5%v/v SF	275.17	51.05
1.0%v/v GTA in 5%v/v SF	273.88	51.45

Appendix C The Electrical Conductivity Measurement of Polycarbazole

The electrical conductivity was measured by using the two-point probe meter connected to a voltage supplier (Keithley, Model 6517a) whose constant voltage can be varied and the current is measured. The regime, where responsive current is linearly proportional to the applied voltage is called the linear Ohmic regime; it can be identified by plotting the applied voltage against the current. The voltage and the current in the regime were converted to the electrical conductivity by the following equation:

$$\sigma = I/\rho = I/(R \times t) = I/(R_s \times V \times t)$$

where σ is the specific conductivity (S/cm)

ρ is the specific resistivity ($\Omega \cdot \text{cm}$)

R_s is the sheet resistance (Ω/sq)

t is the thickness of sample pellet (cm)

V is the applied voltage (V)

I is the measured current (A)

K is the geometric correction factor of the two-point probe meter

($K = 4.29 \times 10^{-4}$).

All sample thicknesses were measured by using a thickness gauge.

Figure C1 shows the electrical conductivity of dedoped and doped PCZ with various mole ratios of the dopant. The result shows the increase in the electrical conductivity with increasing amount of dopant. The maximum value of electrical conductivity is 3.72×10^{-5} S/cm, at $N_{\text{HCl}}: N_{\text{PCZ}}$ to be 100:1. At a higher doping level the electrical conductivity is reduced.

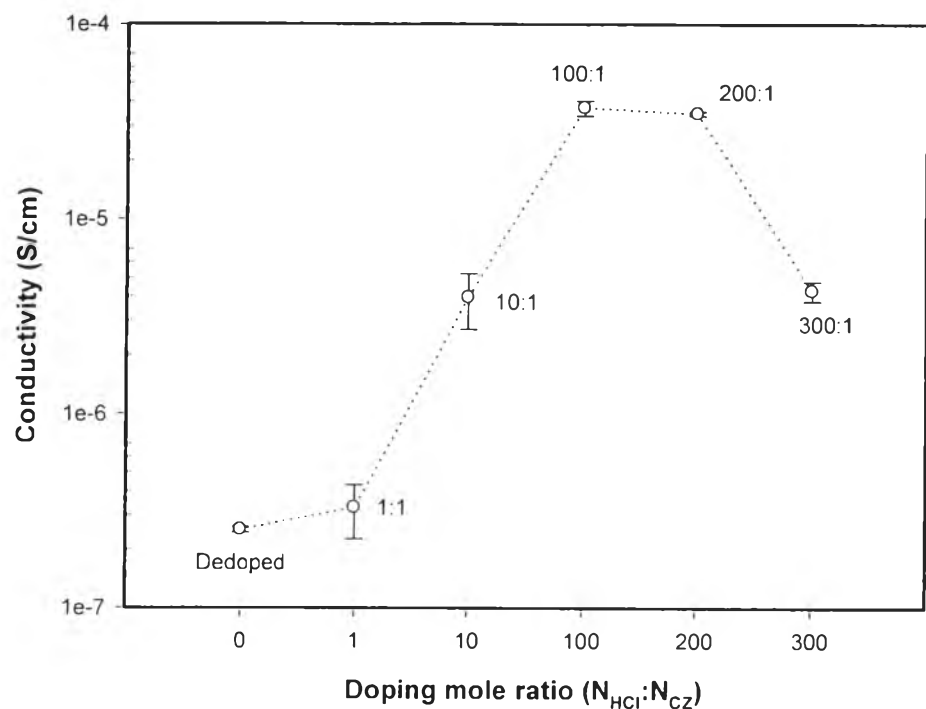


Figure C1 The electrical conductivity of various doping level of polycarbazole.

Table C1 Determination the electrical conductivity (S/cm) of dedoped and doped PCZ

Sample	Electrical conductivity (S/cm)	Standard deviation
Dedoped PCZ	2.53×10^{-7}	9.24×10^{-9}
Doped 1:1 PCZ	3.28×10^{-7}	1.02×10^{-7}
Doped 10:1 PCZ	3.96×10^{-6}	1.26×10^{-6}
Doped 100:1 PCZ	3.72×10^{-5}	3.26×10^{-7}
Doped 200:1 PCZ	3.48×10^{-5}	8.50×10^{-7}
Doped 300:1 PCZ	4.28×10^{-6}	4.90×10^{-7}

Appendix D Density Determination of Polycarbazole

The densities of dedoped and doped 100:1 polycarbazole were determined by the gas pycnometer (Quantachrome, Ultrapycnometer-1000) with a small cell size (7.0699 cm³). The polymer was firstly vacuum-dried for 24 h and then weighted around 1 g at ambient temperature, then loaded into the sample cell. Helium gas was used to purge the sample cell. Density measurements were carried out 10 times for each sample.

Table D1 Density data of dedoped polycarbazole measured at 27 °C

Run	Density (g/cm ³)
1	0.851
2	0.852
3	0.854
4	0.856
5	0.855
6	0.853
7	0.850
8	0.855
9	0.850
10	0.856

Average density	0.854 g/cm ³
Standard deviation	0.002 g/cm ³

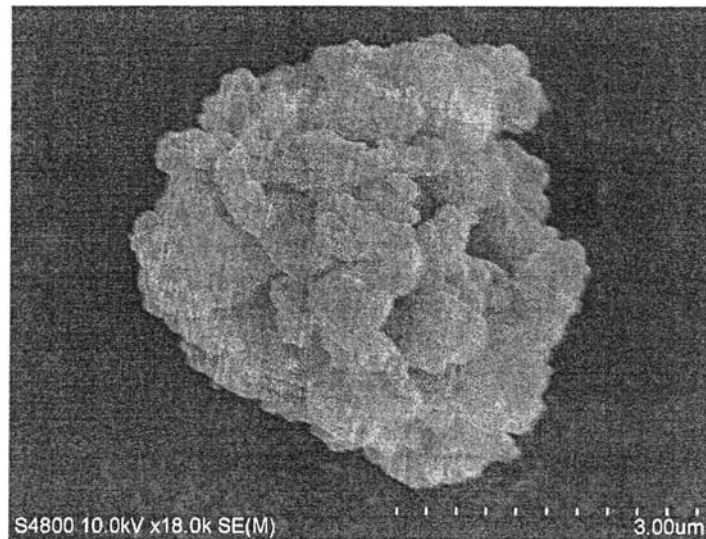
Table D2 Density data of doped 100 :1 polycarbazole measured at 27 °C

Run	Density (g/cm³)
1	1.335
2	1.338
3	1.329
4	1.333
5	1.327
6	1.325
7	1.326
8	1.342
9	1.324
10	1.324

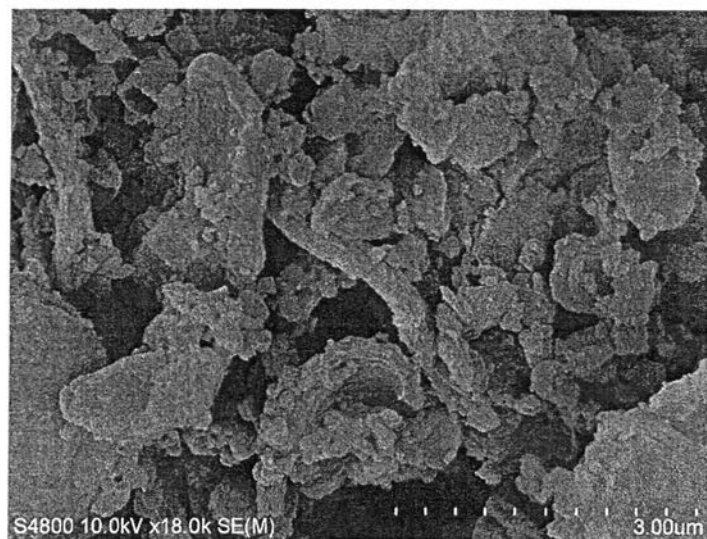
Average density	1.330 g/cm ³
Standard deviation	0.006 g/cm ³

Appendix E Scanning Electron Micrographs of Polycarbazole, Silk Fibroin Hydrogels and Silk Fibroin/Polycarbazole Hydrogels

Scanning electron microscope (Hitachi, S4800) was used to determine the morphological structure.

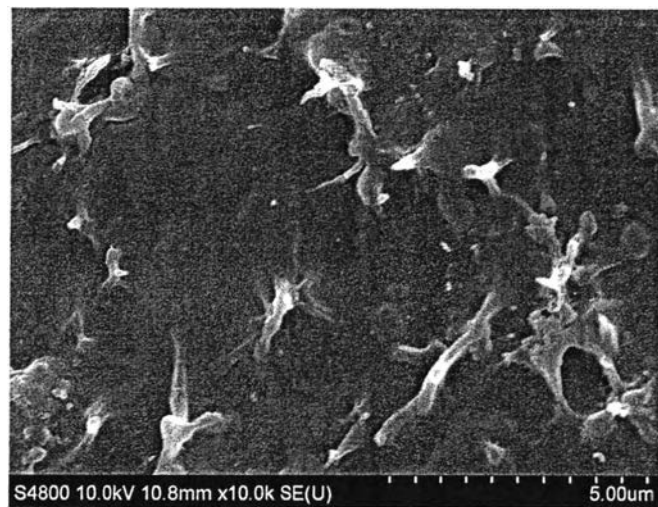


(a)

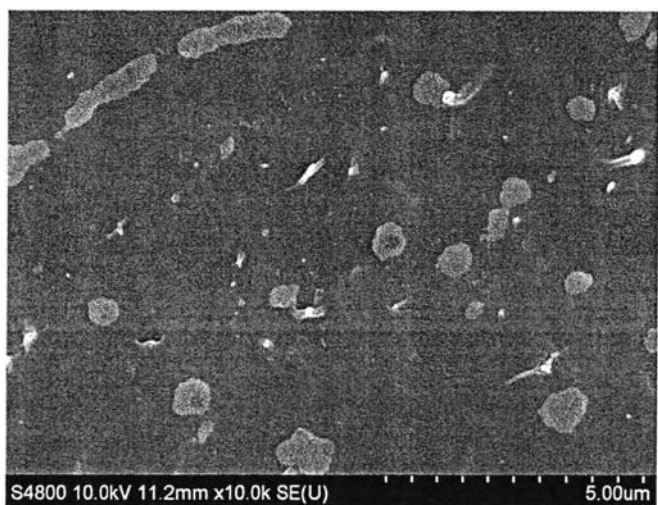


(b)

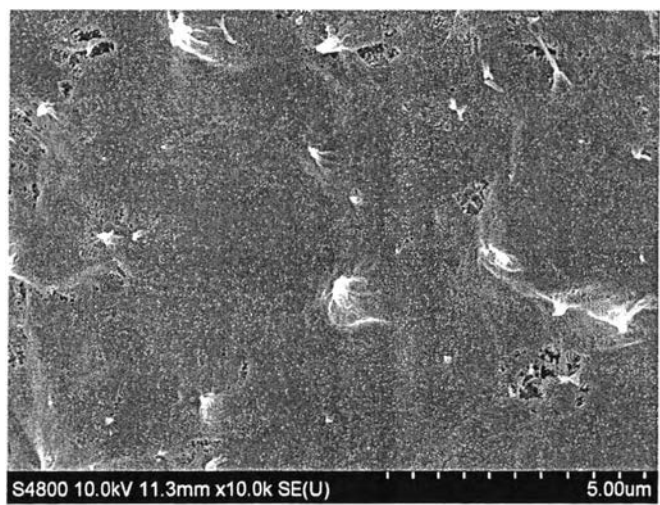
Figure E1 SEM photographs of: (a) dedoped polycarbazole; (b) doped 100 : 1 polycarbazole at magnification of 18000.



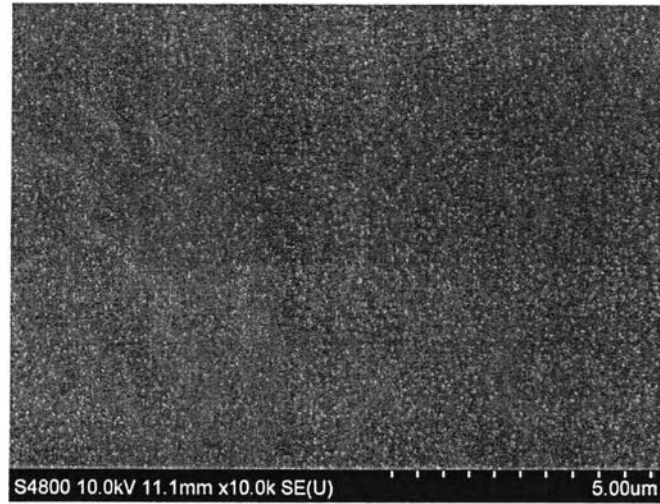
(a)



(b)



(c)



(d)

Figure E2 SEM photographs of dispersion of polycarbazole (PCZ) particle in silk fibroin hyogrogel: (a) 0 vol.%; (b) 0.001 vol.%; (c) 0.01 vol.%; and (d) 0.1 vol.% of PCZ particles.

Appendix F Electromechanical Properties Measurement of Crosslinked Silk Fibroin Hydrogels with Various Amounts of Glutaraldehyde

The electromechanical properties of crosslinked silk fibroin hydrogels were measured by the melt rheometer (Rheometric Scientific, ARES), fixed with a custom-built copper parallel plate fixture with the diameter of 25 mm. DC voltage was applied with a DC power supply (Insteek, GFG 8216A), which can deliver the electric field up to 4 kV/mm. A digital multimeter (Tektronix, CDM 250) was used to monitor the voltage input. The samples were prepared in the sandwich configuration of polyimide-silk fibroin hydrogel-polyimide to prevent the shortening of the circuit. In these experiments, the dynamic strain sweep tests were first carried out to determine appropriate strains by measured the dynamic modulus (G') in linear viscoelastic regime. The following figures, Figure, F1, F2, F3, F4, and F5, show linear viscoelastic regimes of 4 %v/v silk fibroin solution crosslinked with 0.01, 0.05, 0.1, 0.5, and 1.0 %v/v glutaraldehyde, respectively, without electric field strength (0 V/mm). Whereas, Figure, F6, F7, F8, F9, and F10 show linear viscoelastic regimes of 5 %v/v silk fibroin solution crosslinked with 0.01, 0.05, 0.1, 0.5, and 1.0 %v/v glutaraldehyde, respectively, without electric field strength (0 V/mm).

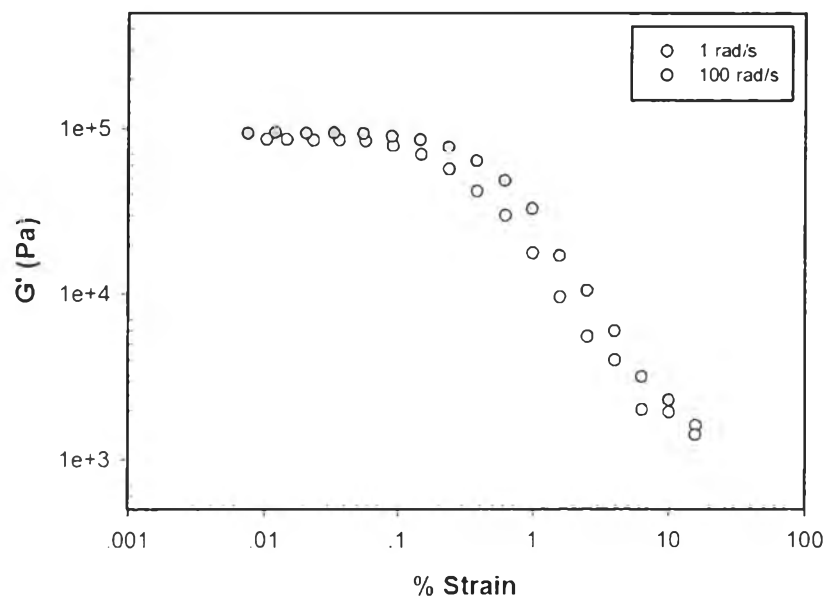


Figure F1 Strain sweep test of 0.01 %v/v glutaraldehyde crosslinked(4 %v/v silk fibroin solution) at frequency 1 rad/s and 100 rad/s, electric field 0 V/mm, sample thickness 1.102 mm, 300 K.

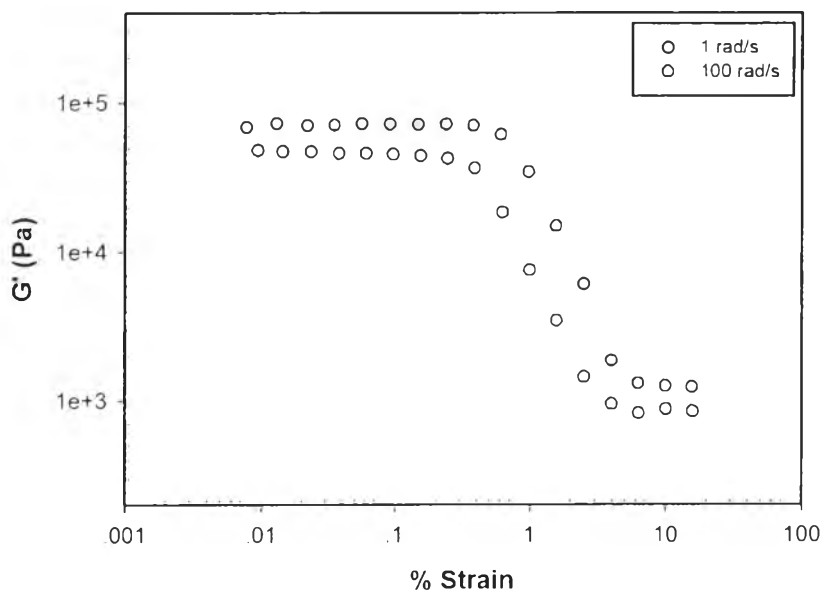


Figure F2 Strain sweep test of 0.05 %v/v glutaraldehyde crosslinked(4 %v/v silk fibroin solution) at frequency 1 rad/s and 100 rad/s, electric field 0 V/mm, sample thickness 1.109 mm, 300 K.

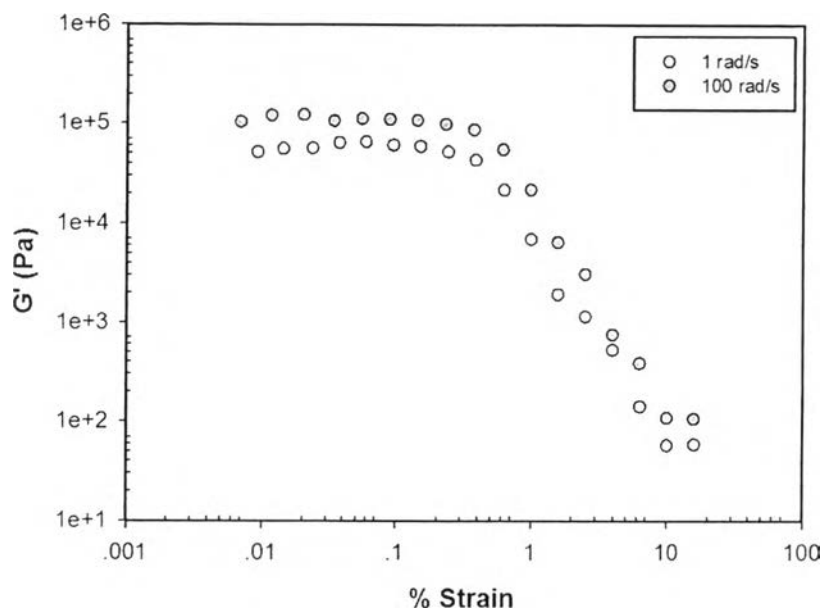


Figure F3 Strain sweep test of 0.1 %v/v glutaraldehyde crosslinked(4 %v/v silk fibroin solution) at frequency 1 rad/s and 100 rad/s, electric field 0 V/mm, sample thickness 1.068 mm, 300 K.

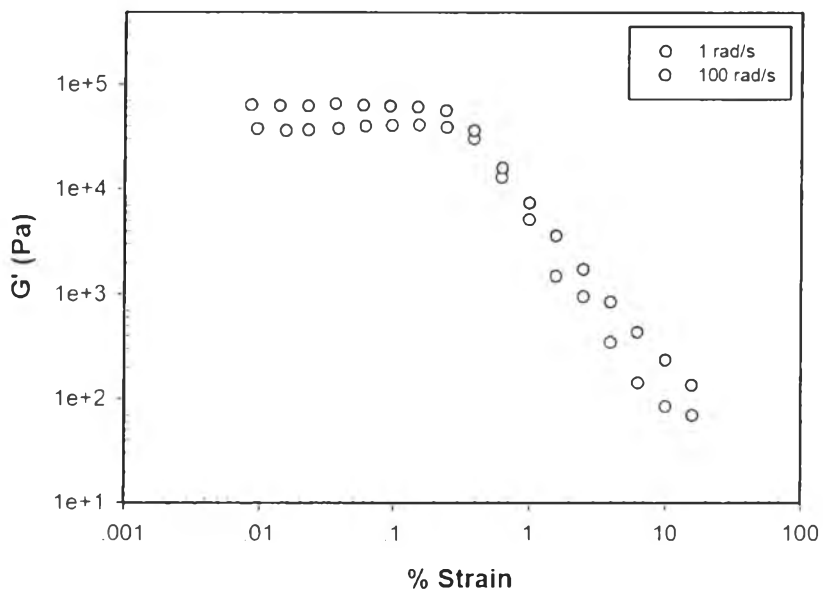


Figure F4 Strain sweep test of 0.5 %v/v glutaraldehyde crosslinked(4 %v/v silk fibroin solution) at frequency 1 rad/s and 100 rad/s, electric field 0 V/mm, sample thickness 1.066 mm, 300 K.

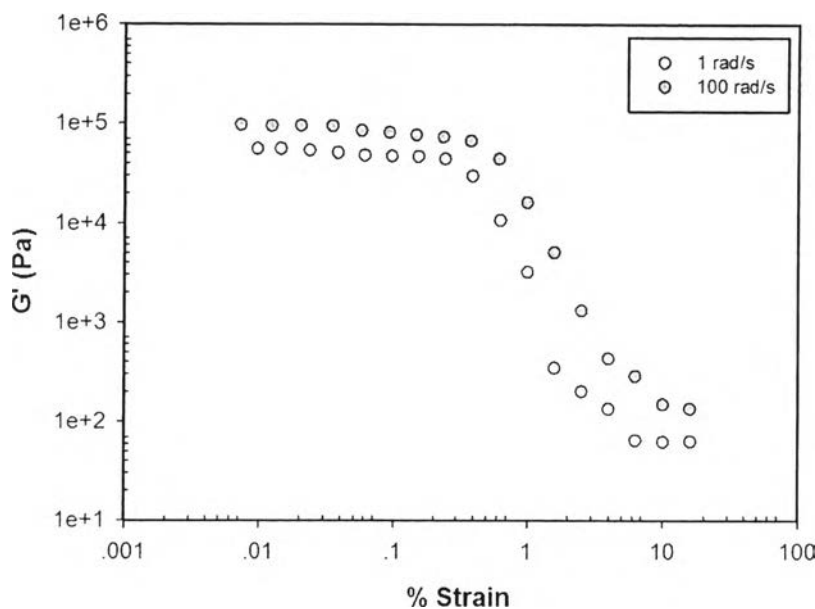


Figure F5 Strain sweep test of 1.0 %v/v glutaraldehyde crosslinked(4 %v/v silk fibroin solution) at frequency 1 rad/s and 100 rad/s, electric field 0 V/mm, sample thickness 1.078 mm, 300 K.

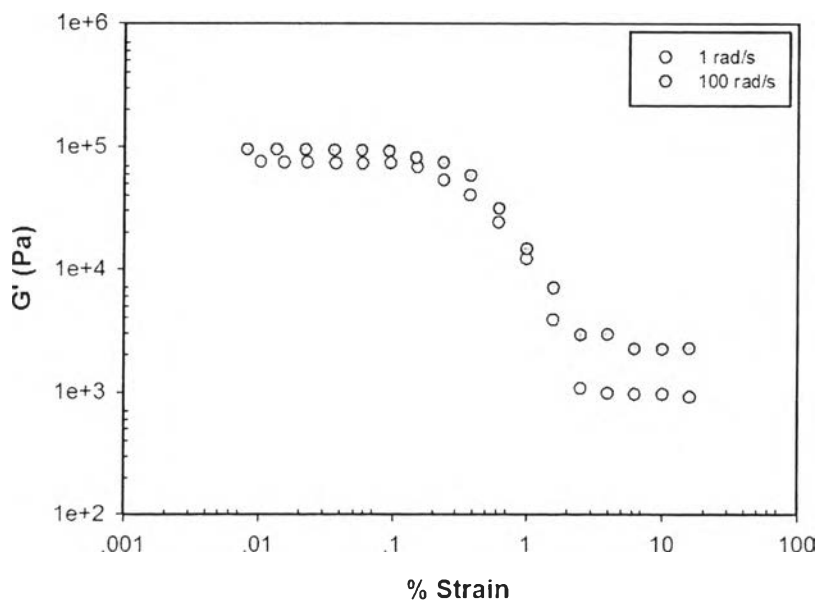


Figure F6 Strain sweep test of 0.01 %v/v glutaraldehyde crosslinked(5 %v/v silk fibroin solution) at frequency 1 rad/s and 100 rad/s, electric field 0 V/mm, sample thickness 1.029 mm, 300 K.

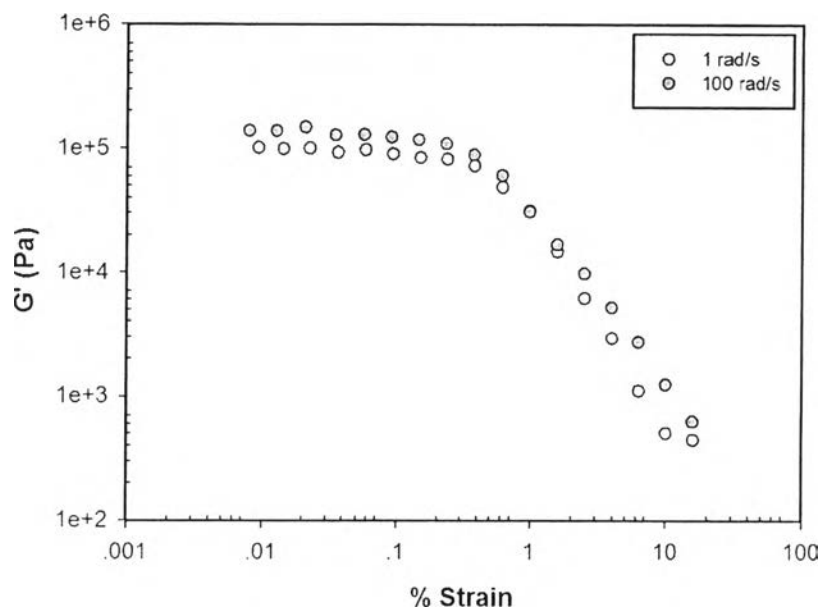


Figure F7 Strain sweep test of 0.05 %v/v glutaraldehyde crosslinked(5 %v/v silk fibroin solution) at frequency 1 rad/s and 100 rad/s, electric field 0 V/mm, sample thickness 1.308 mm, 300 K.

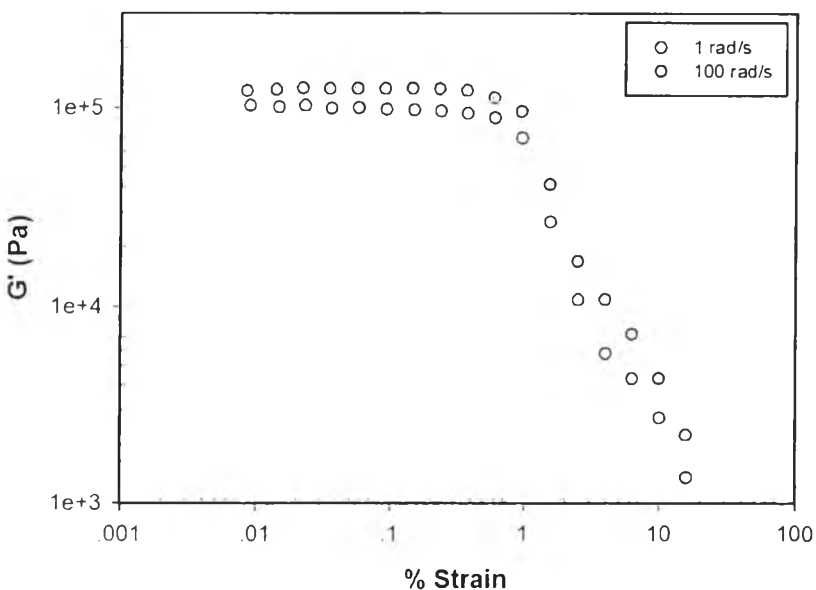


Figure F8 Strain sweep test of 0.1 %v/v glutaraldehyde crosslinked(5 %v/v silk fibroin solution) at frequency 1 rad/s and 100 rad/s, electric field 0 V/mm, sample thickness 1.250 mm, 300 K.

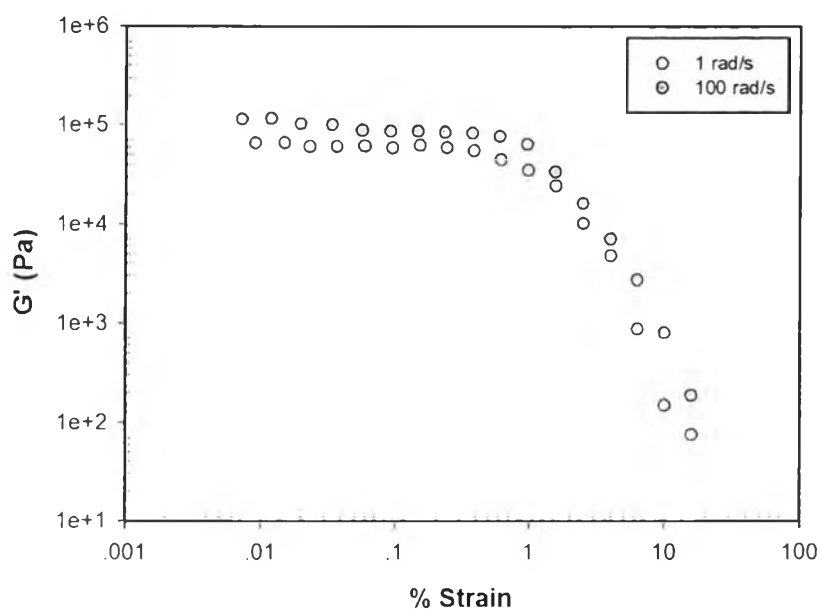


Figure F9 Strain sweep test of 0.5 %v/v glutaraldehyde crosslinked(5 %v/v silk fibroin solution) at frequency 1 rad/s and 100 rad/s, electric field 0 V/mm, sample thickness 1.033 mm, 300 K.

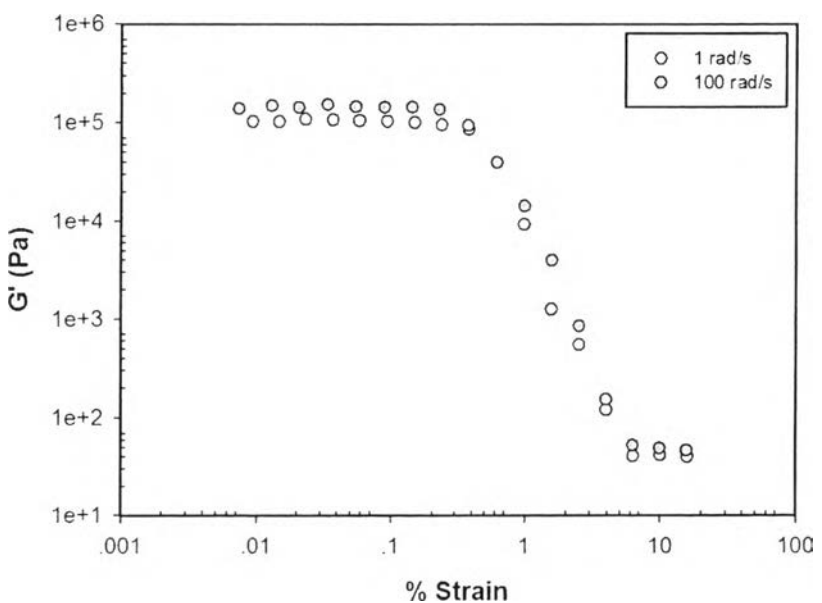


Figure F10 Strain sweep test of 1.0 %v/v glutaraldehyde crosslinked(5 %v/v silk fibroin solution) at frequency 1 rad/s and 100 rad/s, electric field 0 V/mm, sample thickness 1.189 mm, 300 K.

Appendix G Frequency Sweep Test of Crosslinked Silk Fibroin Hydrogels with Various Amounts of Glutaraldehyde; Various Electric Fields

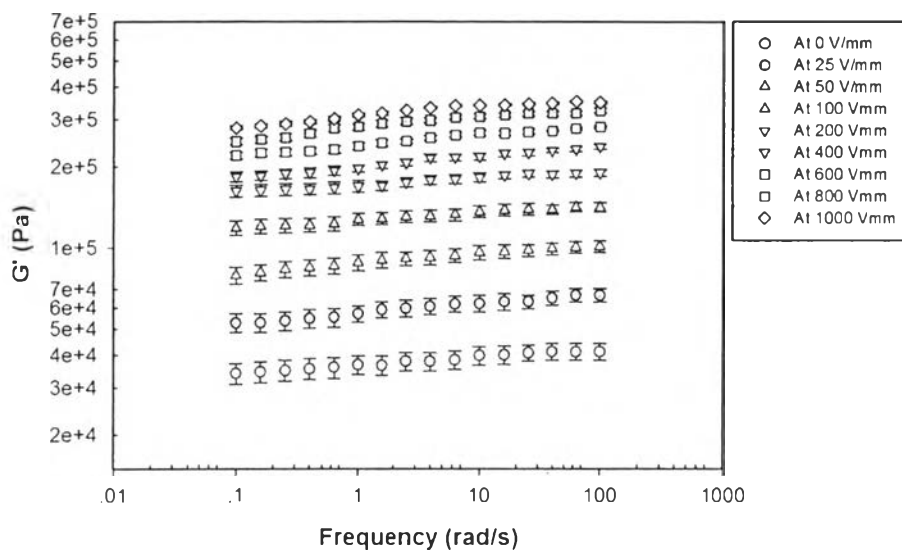


Figure G1 Frequency sweep test of 0.01 %v/v glutaraldehyde crosslinked (4 %v/v silk fibroin solution) at strain 0.03 %, sample thickness 1.102 mm, temperature 300 K.

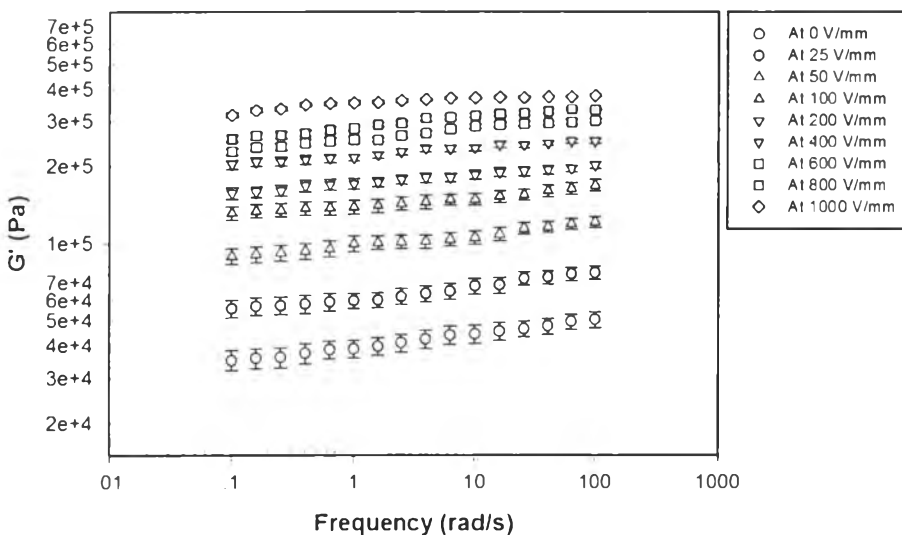


Figure G2 Frequency sweep test of 0.05 %v/v glutaraldehyde crosslinked (4 %v/v silk fibroin solution) at strain 0.05 %, sample thickness 1.109 mm, temperature 300 K.

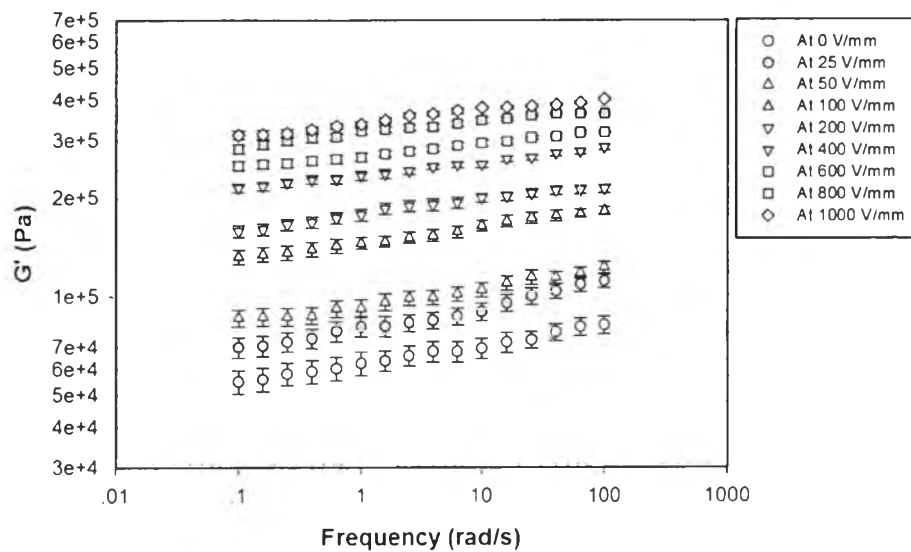


Figure G3 Frequency sweep test of 0.1 %v/v glutaraldehyde crosslinked (4 %v/v silk fibroin solution) at strain 0.06 %, sample thickness 1.068 mm, temperature 300 K.

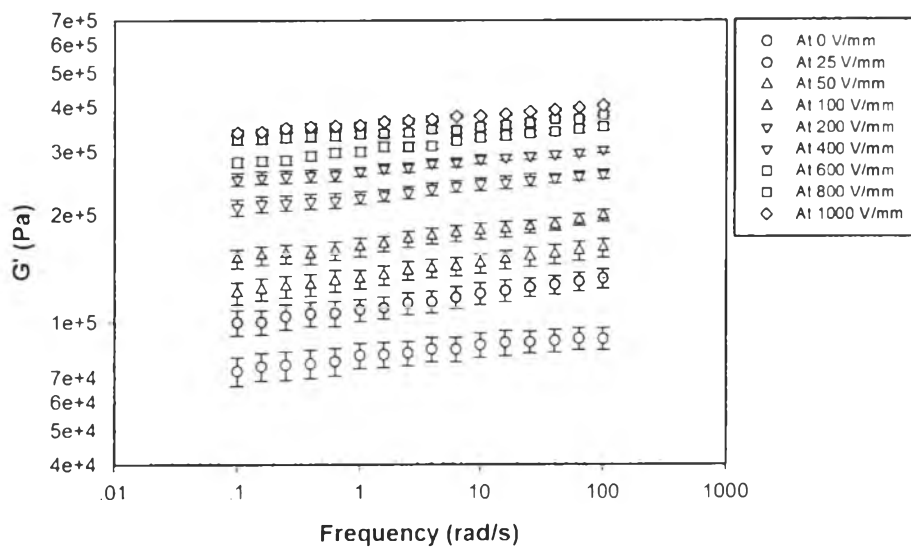


Figure G4 Frequency sweep test of 0.5 %v/v glutaraldehyde crosslinked (4 %v/v silk fibroin solution) at strain 0.10 %, sample thickness 1.066 mm, temperature 300 K.

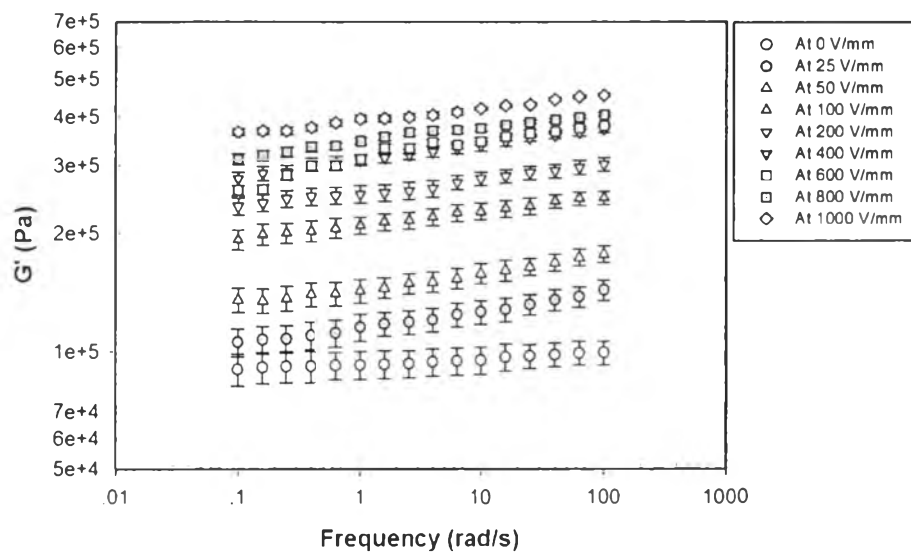


Figure G5 Frequency sweep test of 1.0 %v/v glutaraldehyde crosslinked (4 %v/v silk fibroin solution) at strain 0.10 %, sample thickness 1.078 mm, temperature 300 K.

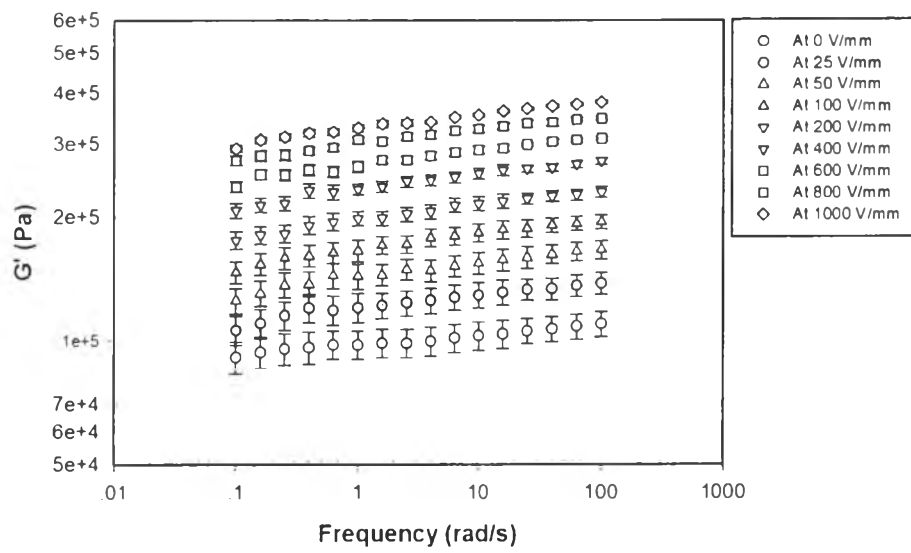


Figure G6 Frequency sweep test of 0.01 %v/v glutaraldehyde crosslinked (5 %v/v silk fibroin solution) at strain 0.10 %, sample thickness 1.029 mm, temperature 300 K.

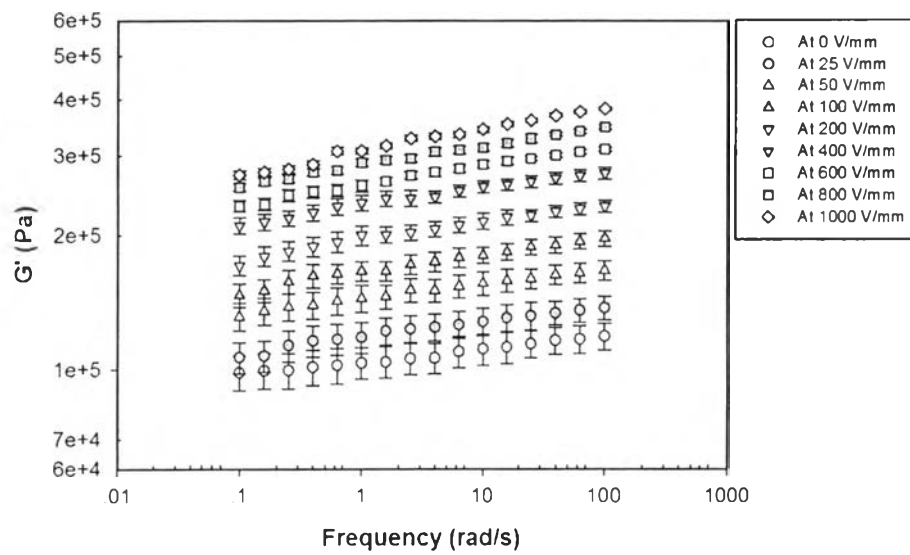


Figure G7 Frequency sweep test of 0.05 %v/v glutaraldehyde crosslinked (5 %v/v silk fibroin solution) at strain 0.10 %, sample thickness 1.308 mm, temperature 300 K.

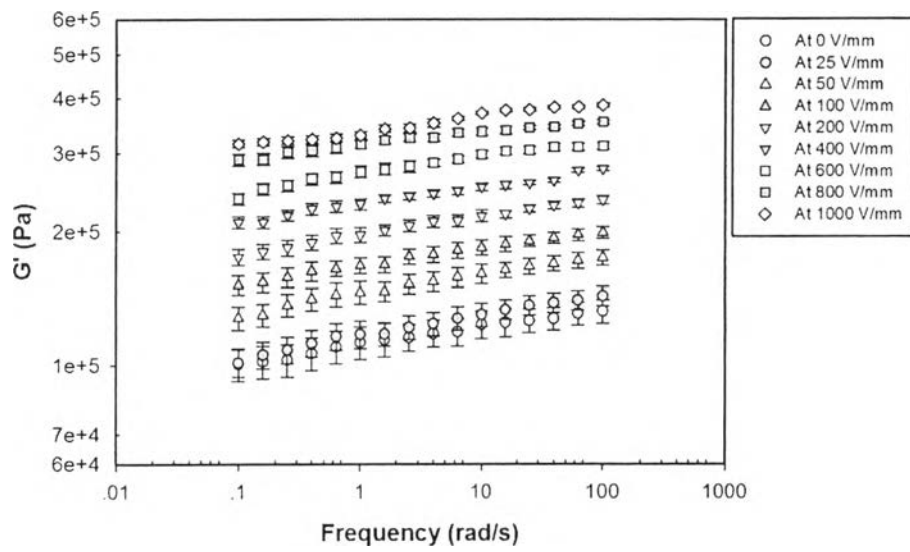


Figure G8 Frequency sweep test of 0.1 %v/v glutaraldehyde crosslinked (5 %v/v silk fibroin solution) at strain 0.15 %, sample thickness 1.250 mm, temperature 300 K.

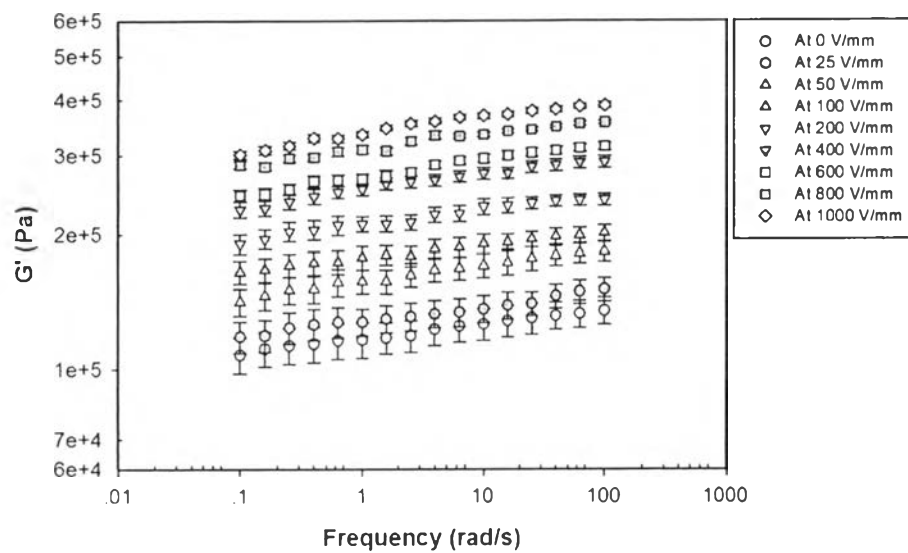


Figure G9 Frequency sweep test of 0.5 %v/v glutaraldehyde crosslinked (5 %v/v silk fibroin solution) at strain 0.15 %, sample thickness 1.033 mm, temperature 300 K.

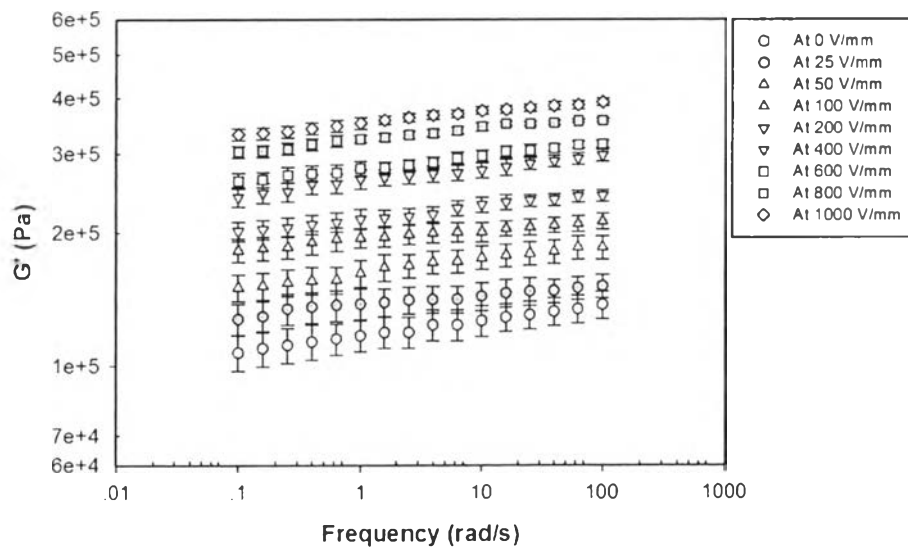


Figure G10 Frequency sweep test of 1.0 %v/v glutaraldehyde crosslinked (5 %v/v silk fibroin solution) at strain 0.15 %, sample thickness 1.198 mm, temperature 300 K.

Appendix H Effect of Electric Field on the Storage Modulus Response ($\Delta G'$) and the Storage Modulus Sensitivity ($\Delta G'/G'_0$) of Crosslinked Silk Fibroin Hydrogels

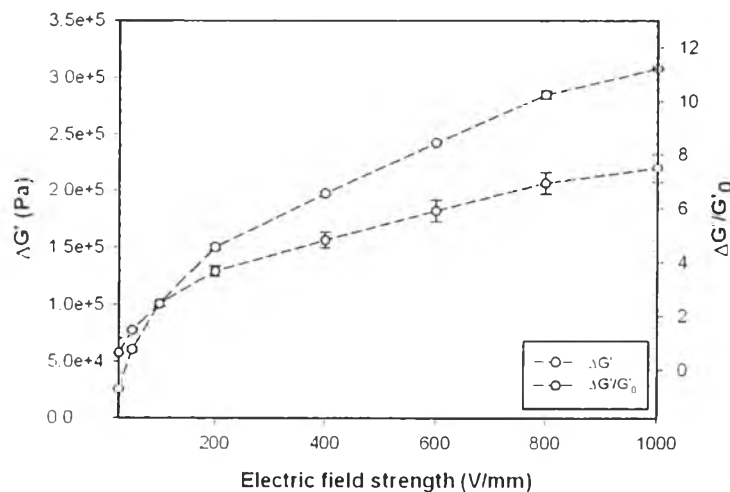


Figure H1 The storage modulus response ($\Delta G'$) and the storage modulus sensitivity ($\Delta G'/G'_0$) versus electric field strength of 0.01 %v/v glutaraldehyde crosslinked (4 %v/v silk fibroin solution) at strain 0.03 %, frequency 100 rad/s, sample thickness 1.102 mm, temperature 300 K.

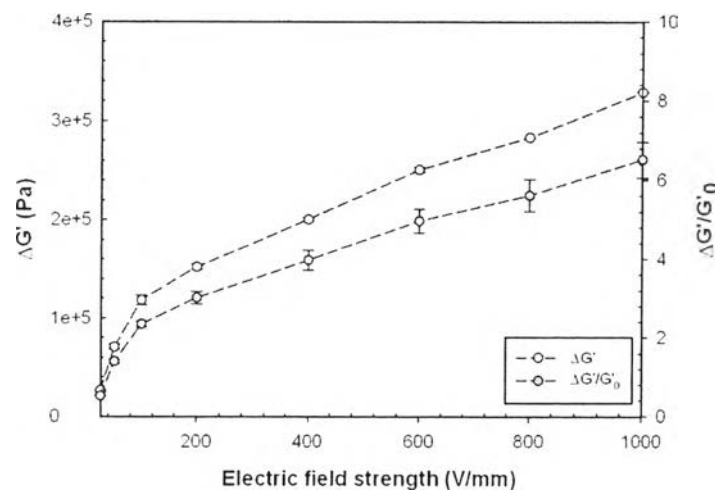


Figure H2 The storage modulus response ($\Delta G'$) and the storage modulus sensitivity ($\Delta G'/G'_0$) versus electric field strength of 0.05 %v/v glutaraldehyde crosslinked (4 %v/v silk fibroin solution) at strain 0.05 %, frequency 100 rad/s, sample thickness 1.109 mm, temperature 300 K

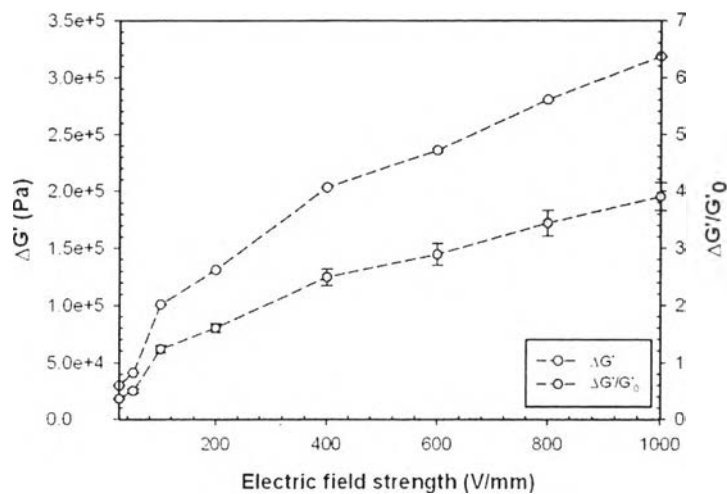


Figure H3 The storage modulus response ($\Delta G'$) and the storage modulus sensitivity ($\Delta G'/G'_0$) versus electric field strength of 0.1 %v/v glutaraldehyde crosslinked (4 %v/v silk fibroin solution) at strain 0.06 %, frequency 100 rad/s, sample thickness 1.068 mm, temperature 300 K.

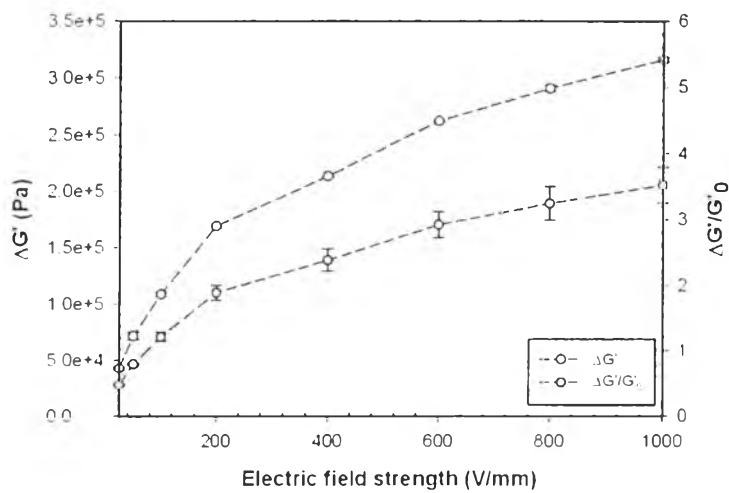


Figure H4 The storage modulus response ($\Delta G'$) and the storage modulus sensitivity ($\Delta G'/G'_0$) versus electric field strength of 0.5 %v/v glutaraldehyde crosslinked (4 %v/v silk fibroin solution) at strain 0.10 %, frequency 100 rad/s, sample thickness 1.066 mm, temperature 300 K.

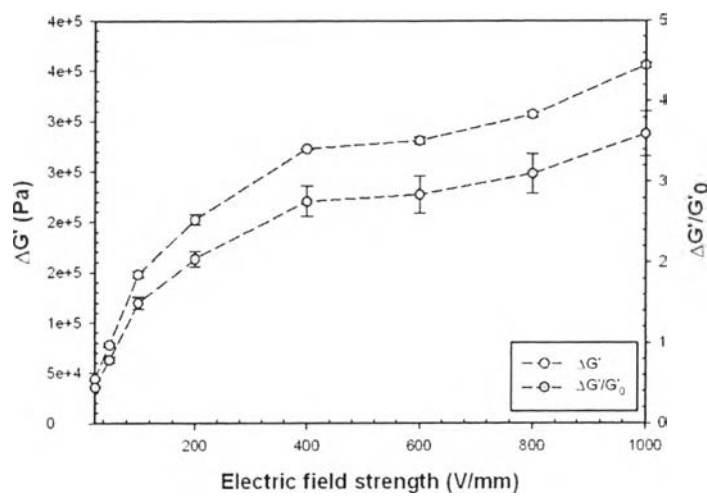


Figure H5 The storage modulus response ($\Delta G'$) and the storage modulus sensitivity ($\Delta G'/G'_0$) versus electric field strength of 1.0 %v/v glutaraldehyde crosslinked (4 %v/v silk fibroin solution) at strain 0.10 %, frequency 100 rad/s, sample thickness 1.078 mm, temperature 300 K.

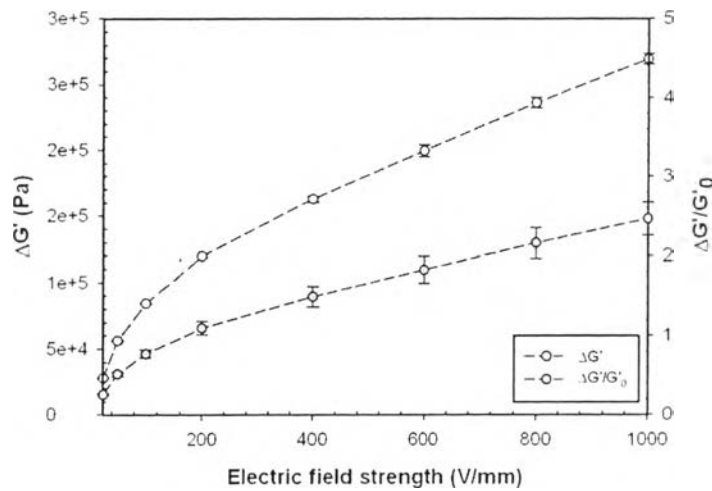


Figure H6 The storage modulus response ($\Delta G'$) and the storage modulus sensitivity ($\Delta G'/G'_0$) versus electric field strength of 0.01 %v/v glutaraldehyde crosslinked (5 %v/v silk fibroin solution) at strain 0.10 %, frequency 100 rad/s, sample thickness 1.029 mm, temperature 300 K.

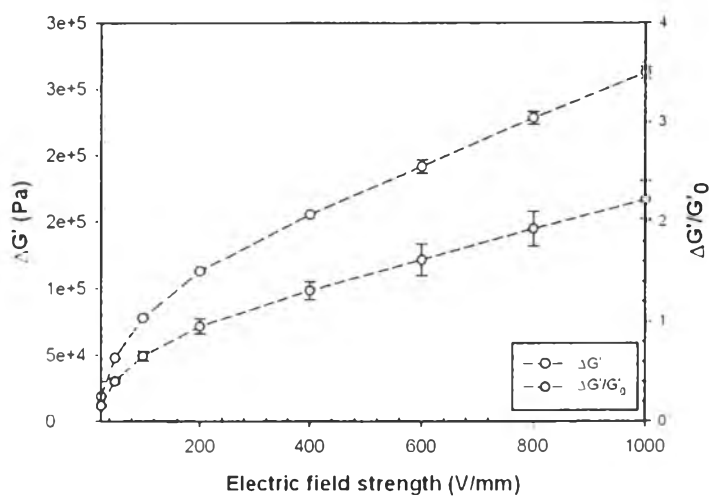


Figure H7 The storage modulus response ($\Delta G'$) and the storage modulus sensitivity ($\Delta G'/G'_0$) versus electric field strength of 0.05 %v/v glutaraldehyde crosslinked (5 %v/v silk fibroin solution) at strain 0.10 %, frequency 100 rad/s, sample thickness 1.308 mm, temperature 300 K.

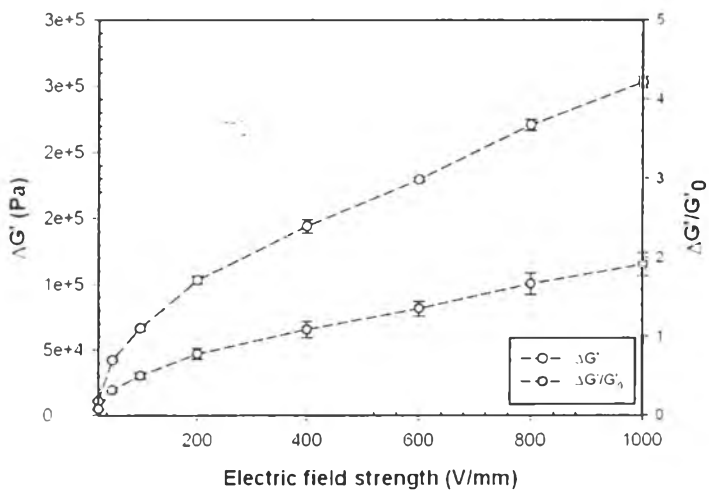


Figure H8 The storage modulus response ($\Delta G'$) and the storage modulus sensitivity ($\Delta G'/G'_0$) versus electric field strength of 0.1 %v/v glutaraldehyde crosslinked (5 %v/v silk fibroin solution) at strain 0.15 %, frequency 100 rad/s, sample thickness 1.250 mm, temperature 300 K.

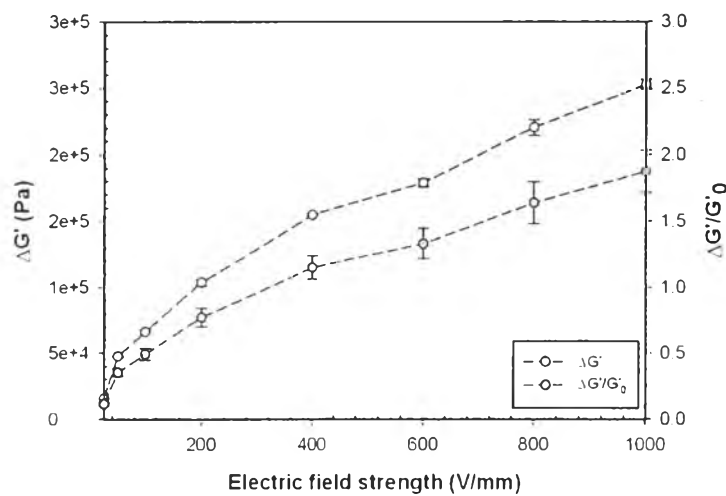


Figure H9 The storage modulus response ($\Delta G'$) and the storage modulus sensitivity ($\Delta G'/G'_0$) versus electric field strength of 0.5 %v/v glutaraldehyde crosslinked (5 %v/v silk fibroin solution) at strain 0.15 %, frequency 100 rad/s, sample thickness 1.033 mm, temperature 300 K.

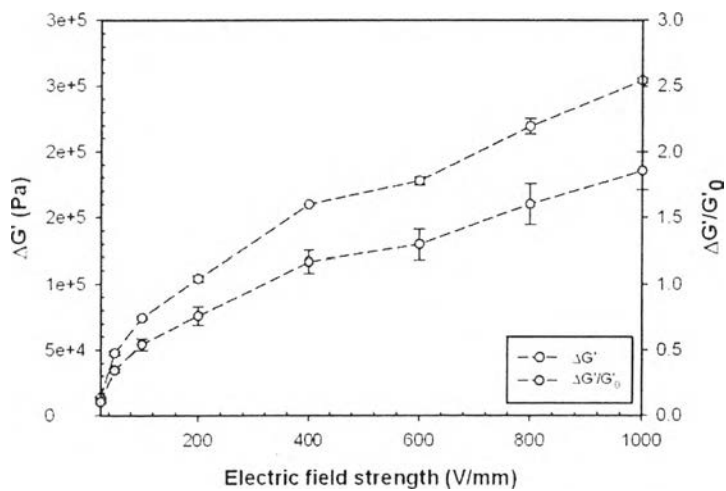


Figure H10 The storage modulus response ($\Delta G'$) and the storage modulus sensitivity ($\Delta G'/G'_0$) versus electric field strength of 1.0 %v/v glutaraldehyde crosslinked (5 %v/v silk fibroin solution) at strain 0.15 %, frequency 100 rad/s, sample thickness 1.198 mm, temperature 300 K.

Table H1 Comparison of the storage modulus responses and the storage modulus sensitivities of crosslinked silk fibroin (SF) hydrogels

Materials	Glutaraldehyde (%v/v)	Electric field strength (V/mm)	Frequency (rad/s)	Temperature (K)	Storage modulus response $(\Delta G')$ (Pa)	Initial storage modulus (G'_0) (Pa)	Storage modulus sensitivity $(\Delta G'/ G'_0)$
4 %v/v SF solution	0.01	1000	100	300	3.08×10^5	4.12×10^4	7.48
	0.05				3.28×10^5	5.05×10^4	6.50
	0.10				3.18×10^5	8.18×10^4	3.89
	0.50				3.15×10^5	9.00×10^4	3.50
	1.00				3.45×10^5	9.93×10^4	3.47
5 %v/v SF solution	0.01			300	2.70×10^5	1.10×10^5	2.45
	0.05				2.63×10^5	1.19×10^5	2.21
	0.10				2.54×10^5	1.33×10^5	1.91
	0.50				2.49×10^5	1.35×10^5	1.87
	1.00				2.55×10^5	1.38×10^5	1.85

Appendix I Electromechanical Properties Measurements of Silk Fibroin/Polycarbazole Composites

The electromechanical properties of the composite hydrogels were carried out by melt rheometer (Rheometric Scientific, ARES). It was fitted with a custom-built copper parallel plates fixture, diameter 25 mm. A DC voltage was applied by DC power supply (Insteek, GFG 8216A), which can deliver electric field strength to 600 V/mm. A digital multimeter was used to monitor the voltage input. Dynamic strain sweep test was first carried out to determine appropriate strains by measured G' in viscoelastic regime. The following figures, Figure I1, I2, I3, I4, I5, and I6, showed linear viscoelastic regimes of the silk fibroin/polycarbazole hydrogels with various polycarbazole concentrations, respectively.

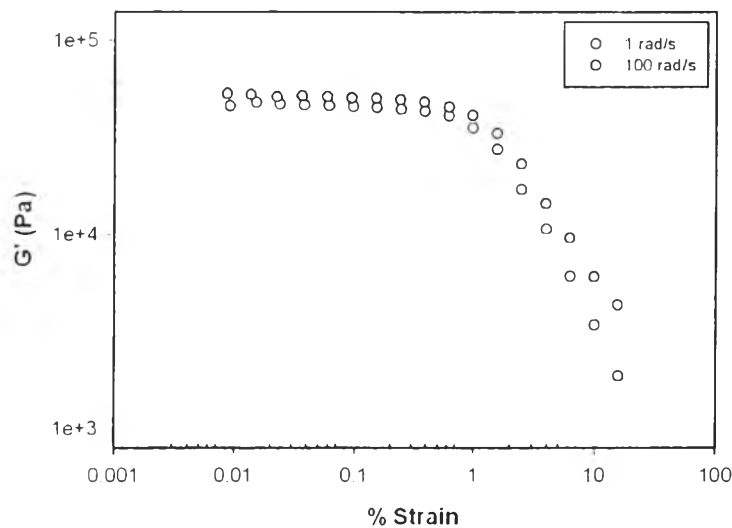


Figure I1 Strain sweep test of silk fibroin/polycarbazole (0.001 %v/v of polycarbazole) hydrogel at frequency 1 rad/s and 100 rad/s, electric field 0 V/mm, sample thickness 1.251 mm, temperature 300 K.

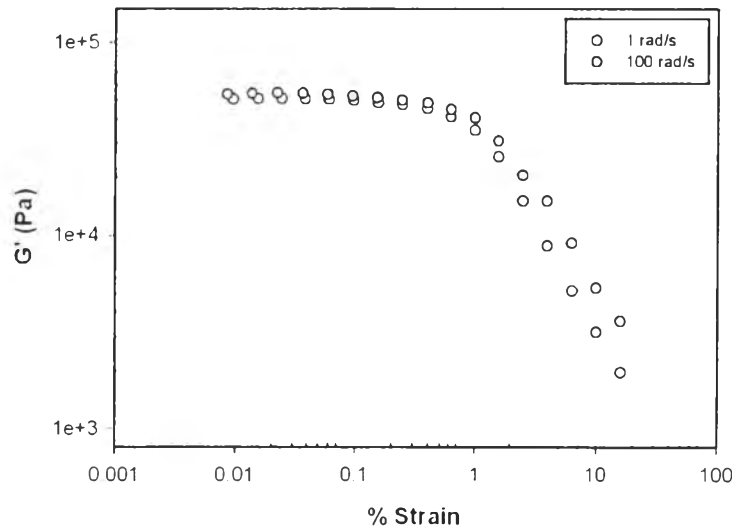


Figure I2 Strain sweep test of silk fibroin/polycarbazole (0.005 %v/v of polycarbazole) hydrogel at frequency 1 rad/s and 100 rad/s, electric field 0 V/mm, sample thickness 1.678 mm, temperature 300 K.

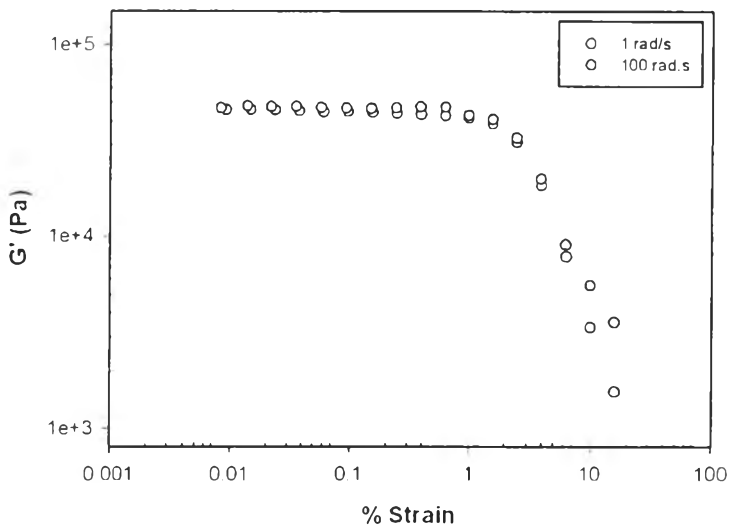


Figure I3 Strain sweep test of silk fibroin/polycarbazole (0.01 %v/v of polycarbazole) hydrogel at frequency 1 rad/s and 100 rad/s, electric field 0 V/mm, sample thickness 1.432 mm, temperature 300 K.

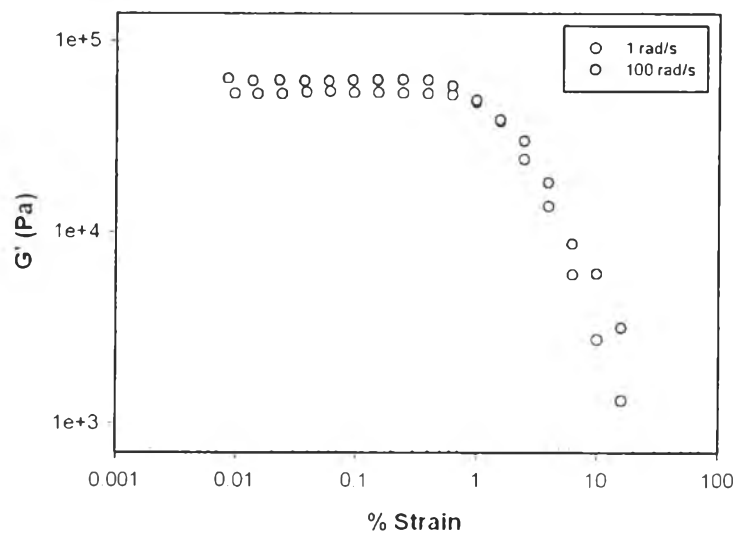


Figure 14 Strain sweep test of silk fibroin/polycarbazole (0.05 %v/v of polycarbazole) hydrogel at frequency 1 rad/s and 100 rad/s, electric field 0 V/mm, sample thickness 1.668 mm, temperature 300 K.

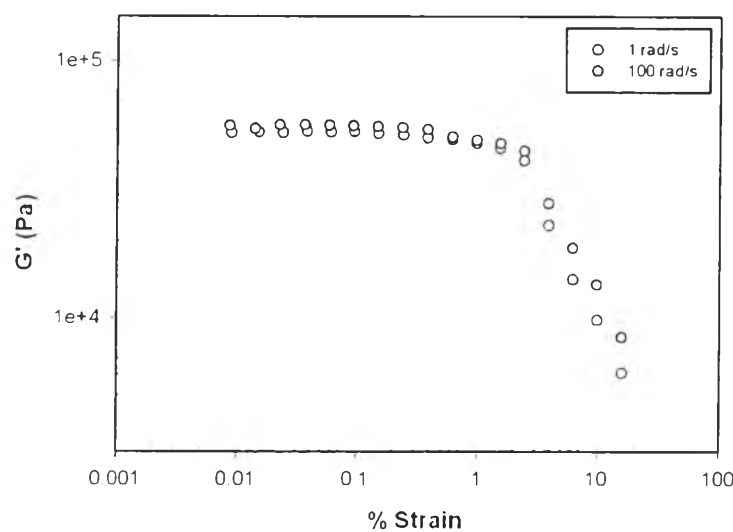


Figure 15 Strain sweep test of silk fibroin/polycarbazole (0.1 %v/v of polycarbazole) hydrogel at frequency 1 rad/s and 100 rad/s, electric field 0 V/mm, sample thickness 1.235 mm, temperature 300 K.

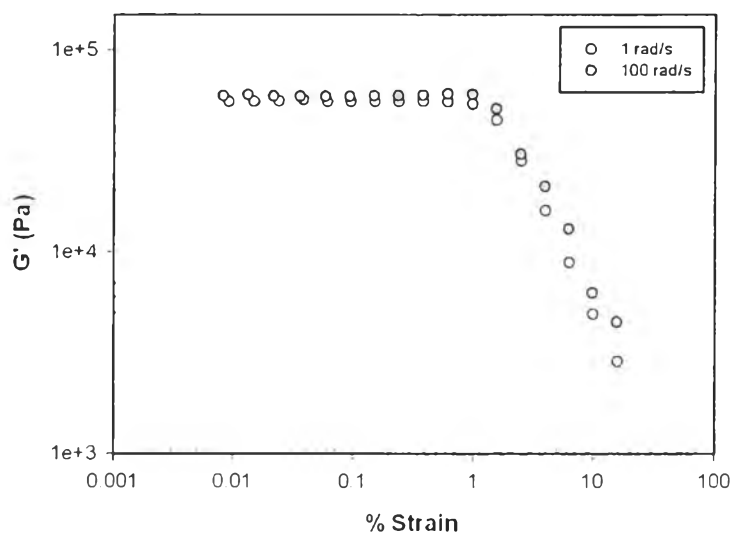


Figure I6 Strain sweep test of silk fibroin/polycarbazole (0.5 %v/v of polycarbazole) hydrogel at frequency 1 rad/s and 100 rad/s, electric field 0 V/mm, sample thickness 1.379 mm, temperature 300 K.

Appendix J Frequency Sweep Test of Silk Fibroin/Polycarbazole Composites; Various Electric Fields

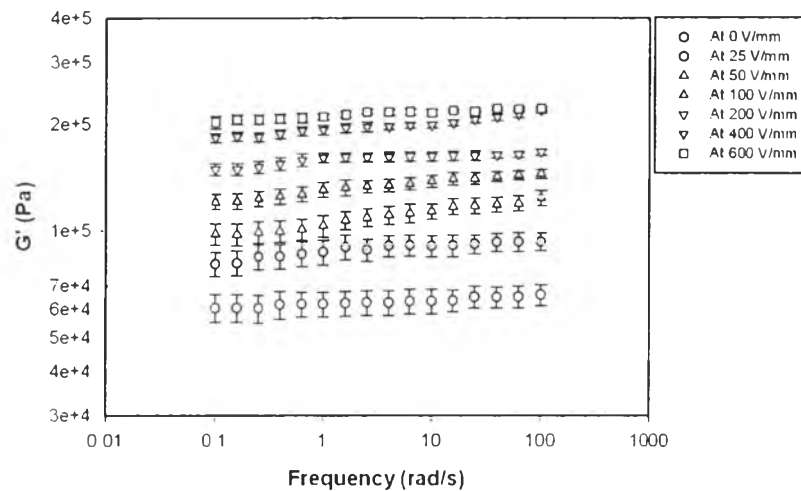


Figure J1 Frequency sweep test of silk fibroin/polycarbazole (0.001 %v/v of polycarbazole) hydrogel at strain 0.15 %, sample thickness 1.251 mm, temperature 300 K.

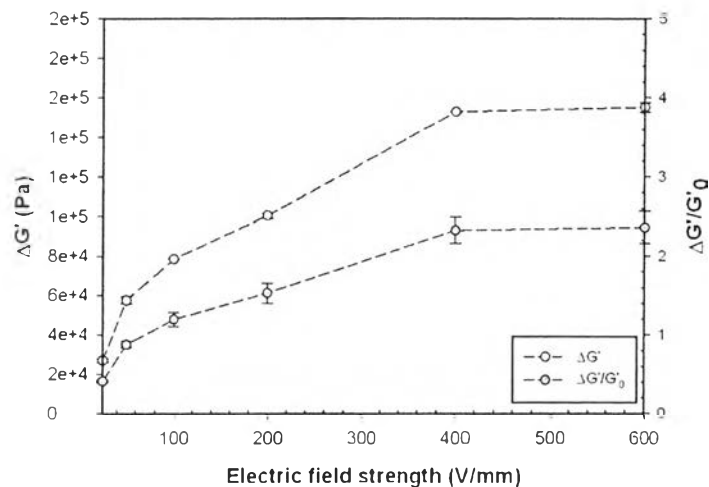


Figure J2 The storage modulus response ($\Delta G'$) and the storage modulus sensitivity ($\Delta G'/G'_0$) versus electric field strength of silk fibroin/polycarbazole (0.001 %v/v of polycarbazole) hydrogel at strain 0.15 %, frequency 100 rad/s, sample thickness 1.251 mm, temperature 300 K.

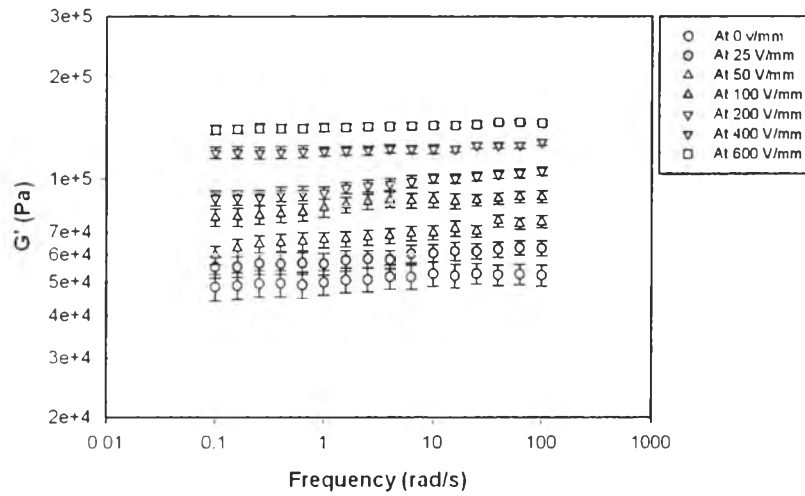


Figure J3 Frequency sweep test of silk fibroin/polycarbazole (0.005 %v/v of polycarbazole) hydrogel at strain 0.15 %, sample thickness 1.678 mm, temperature 300 K.

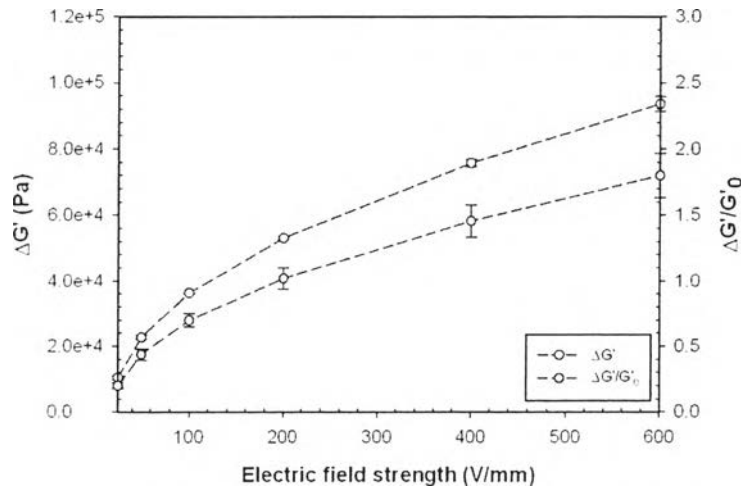


Figure J4 The storage modulus response ($\Delta G'$) and the storage modulus sensitivity ($\Delta G'/G'_0$) versus electric field strength of silk fibroin/polycarbazole (0.005 %v/v of polycarbazole) hydrogel at strain 0.15 %, frequency 100 rad/s, sample thickness 1.678 mm, temperature 300 K.

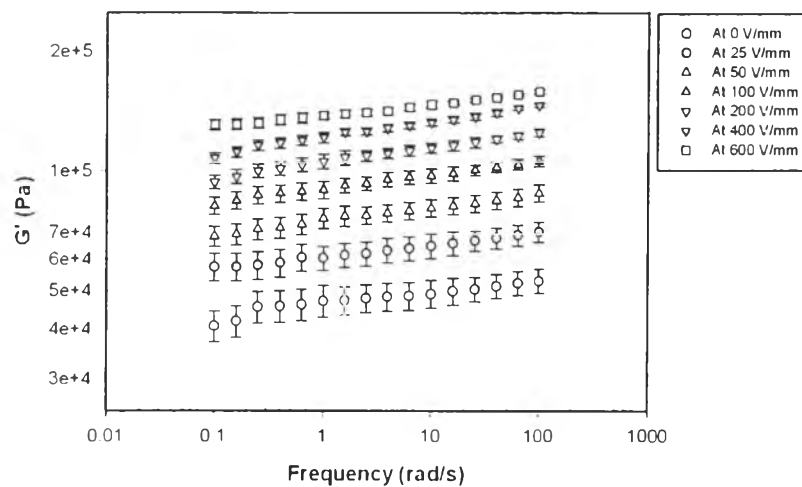


Figure J5 Frequency sweep test of silk fibroin/polycarbazole (0.01 %v/v of polycarbazole) hydrogel at strain 0.15 %, sample thickness 1.432 mm, temperature 300 K.

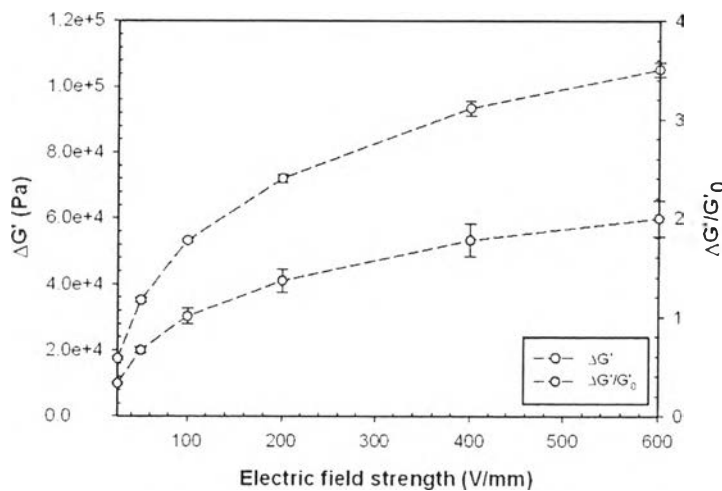


Figure J6 The storage modulus response ($\Delta G'$) and the storage modulus sensitivity ($\Delta G'/G'_0$) versus electric field strength of silk fibroin/polycarbazole (0.01 %v/v of polycarbazole) hydrogel at strain 0.15 %, frequency 100 rad/s, sample thickness 1.432 mm, temperature 300 K.

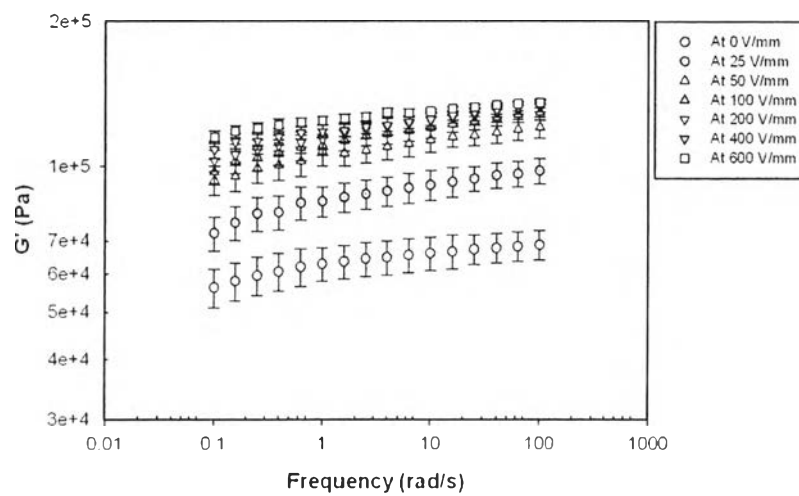


Figure J7 Frequency sweep test of silk fibroin/polycarbazole (0.05 %v/v of polycarbazole) hydrogel at strain 0.15 %, sample thickness 1.668 mm, temperature 300 K.

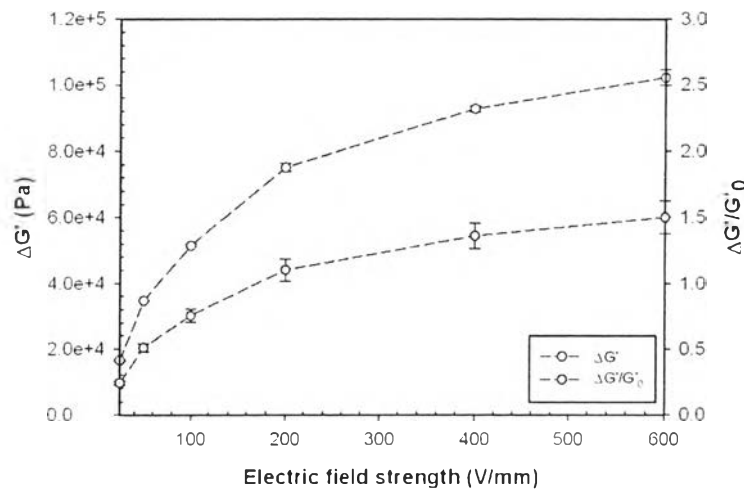


Figure J8 The storage modulus response ($\Delta G'$) and the storage modulus sensitivity ($\Delta G'/G'_0$) versus electric field strength of silk fibroin/polycarbazole (0.05 %v/v of polycarbazole) hydrogel at strain 0.15 %, frequency 100 rad/s, sample thickness 1.668 mm, temperature 300 K.

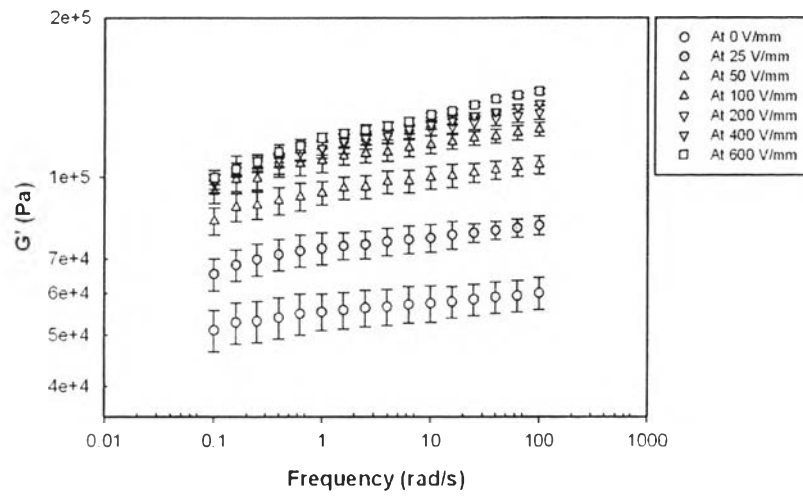


Figure J9 Frequency sweep test of silk fibroin/polycarbazole (0.1 %v/v of polycarbazole) hydrogel at strain 0.15 %, sample thickness 1.235 mm, temperature 300 K.

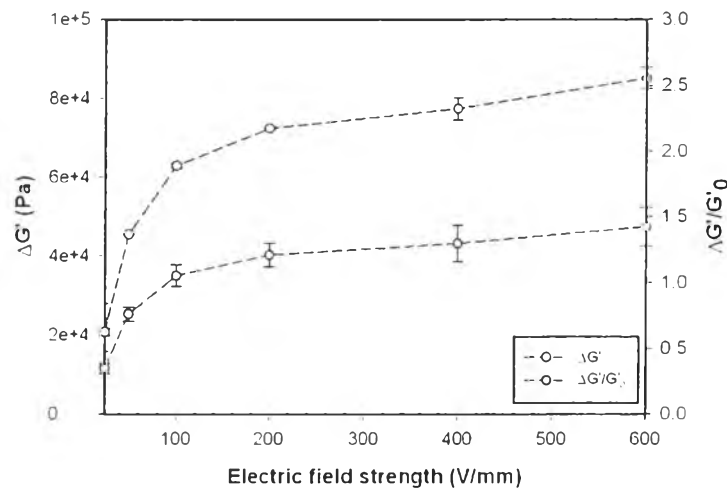


Figure J10 The storage modulus response ($\Delta G'$) and the storage modulus sensitivity ($\Delta G'/G'_0$) versus electric field strength of silk fibroin/polycarbazole (0.1 %v/v of polycarbazole) hydrogel at strain 0.15 %, frequency 100 rad/s, sample thickness 1.235 mm, temperature 300 K.

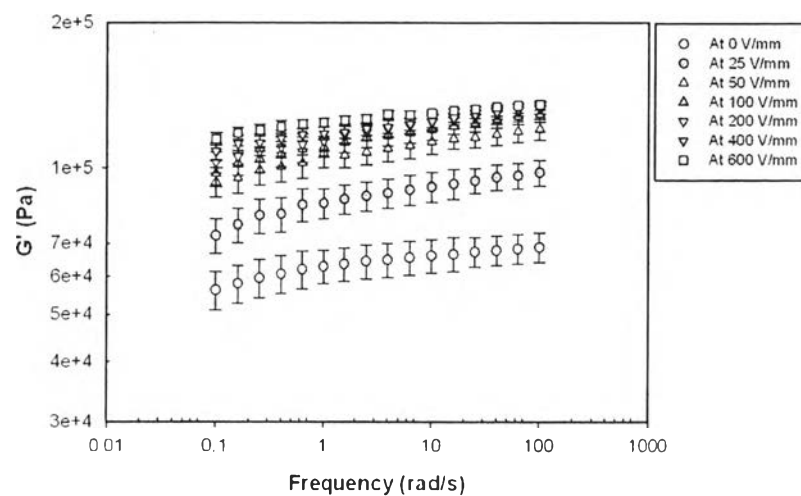


Figure J11 Frequency sweep test of silk fibroin/polycarbazole (0.5 %v/v of polycarbazole) hydrogel at strain 0.15 %, sample thickness 1.379 mm, temperature 300 K.

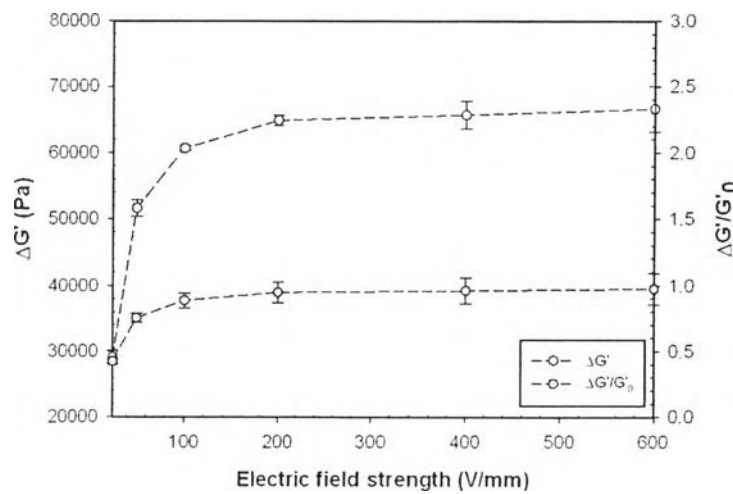


Figure J12 The storage modulus response ($\Delta G'$) and the storage modulus sensitivity ($\Delta G'/G'_0$) versus electric field strength of silk fibroin/polycarbazole (0.5 %v/v of polycarbazole) hydrogel at strain 0.15 %, frequency 100 rad/s, sample thickness 1.251 mm, temperature 300 K.

Table J1 The storage modulus responses and the storage modulus sensitivities of silk fibroin/polycarbazole (SF/PCZ) composites

Material	PCZ (%v/v)	Electric field strength (V/mm)	Frequency (rad/s)	Temperature (K)	Storage modulus response $(\Delta G')$ (Pa)	Initial storage modulus (G'_{0}) (Pa)	Storage modulus sensitivity $(\Delta G'/ G'_{0})$
SF/PCZ	0	600	100	300	2.42×10^5	4.12×10^4	5.87
SF/PCZ	0.001				1.62×10^5	5.88×10^4	2.75
SF/PCZ	0.005				9.36×10^4	5.23×10^4	1.79
SF/PCZ	0.01				9.72×10^4	6.09×10^4	1.60
SF/PCZ	0.05				1.02×10^5	6.83×10^4	1.50
SF/PCZ	0.1				7.72×10^4	6.81×10^4	1.33
SF/PCZ	0.5				6.66×10^4	6.87×10^4	0.97

Appendix K Electromechanical Properties Measurements of Silk Fibroin/Dedoped Polycarbazole Composites

The electromechanical properties of the composite hydrogels were carried out by melt rheometer (Rheometric Scientific, ARES). It was fitted with a custom-built copper parallel plates fixture, diameter 25 mm. A DC voltage was applied by DC power supply (Insteek, GFG 8216A), which can deliver electric field strength to 600 V/mm. A digital multimeter was used to monitor the voltage input. Dynamic strain sweep test was first carried out to determine appropriate strains by measured G' in viscoelastic regime. The following figures, Figure K1, K2, and K3, showed linear viscoelastic regimes of the silk fibroin/polycarbazole hydrogels with various polycarbazole concentrations, respectively.

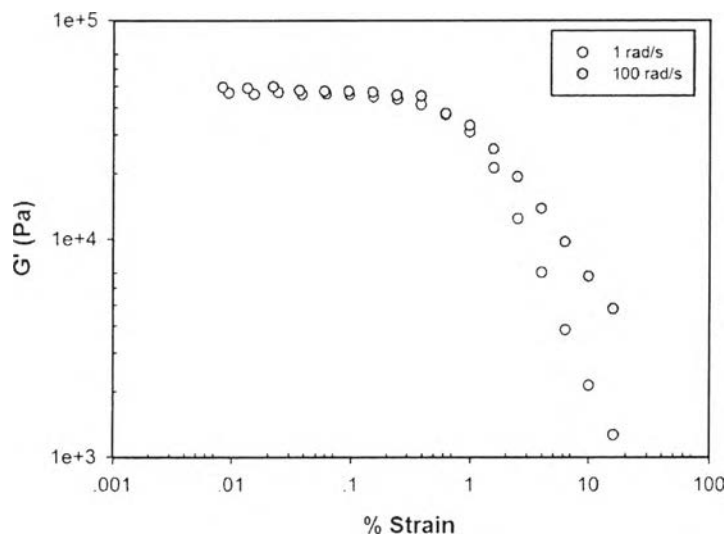


Figure K1 Strain sweep test of silk fibroin/dedoped polycarbazole (0.001 %v/v of polycarbazole) hydrogel at frequency 1 rad/s and 100 rad/s, electric field 0 V/mm, sample thickness 1.353 mm, temperature 300 K.

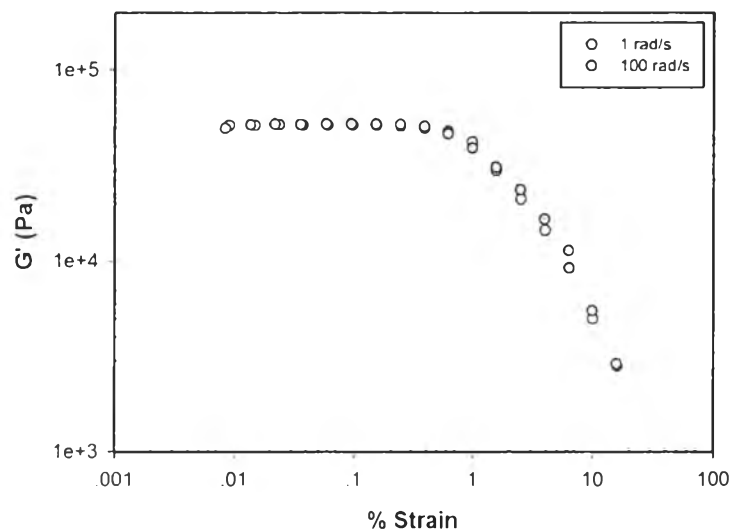


Figure K2 Strain sweep test of silk fibroin/dedoped polycarbazole (0.01 %v/v of polycarbazole) hydrogel at frequency 1 rad/s and 100 rad/s, electric field 0 V/mm, sample thickness 1.424 mm, temperature 300 K.

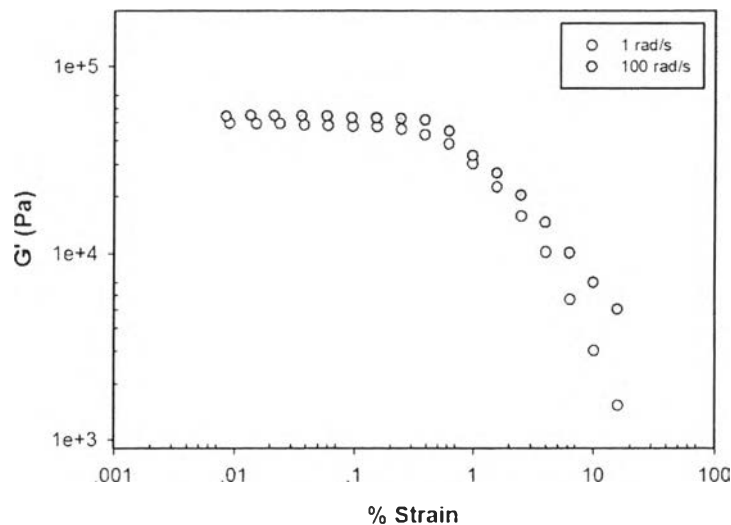


Figure K3 Strain sweep test of silk fibroin/dedoped polycarbazole (0.1 %v/v of polycarbazole) hydrogel at frequency 1 rad/s and 100 rad/s, electric field 0 V/mm, sample thickness 1.383 mm, temperature 300 K.

Appendix L Frequency Sweep Test of Silk Fibroin/Dedoped Polycarbazole Composites; Various Electric Fields

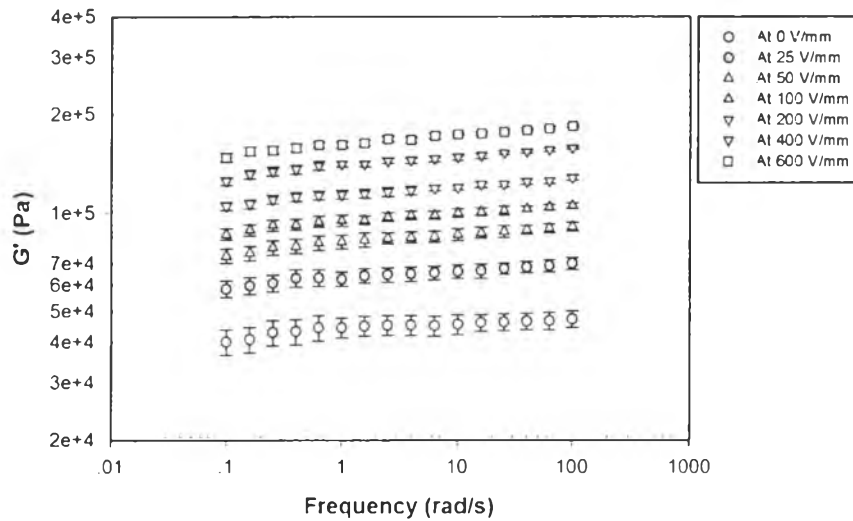


Figure L1 Frequency sweep test of silk fibroin/dedoped polycarbazole (0.001 %v/v of polycarbazole) hydrogel at strain 0.1 %, sample thickness 1.353 mm, temperature 300 K.

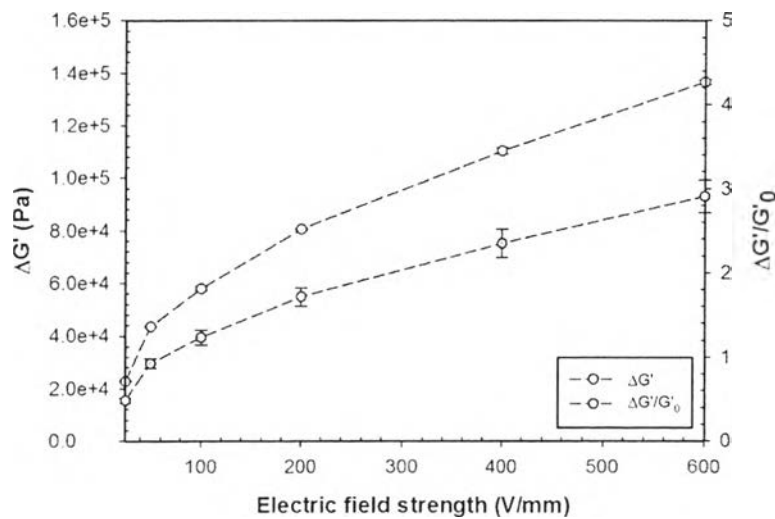


Figure L2 The storage modulus response ($\Delta G'$) and the storage modulus sensitivity ($\Delta G'/G'_0$) versus electric field strength of silk fibroin/dedoped polycarbazole (0.001 %v/v of polycarbazole) hydrogel at strain 0.1 %, frequency 100 rad/s, sample thickness 1.353 mm, temperature 300 K.

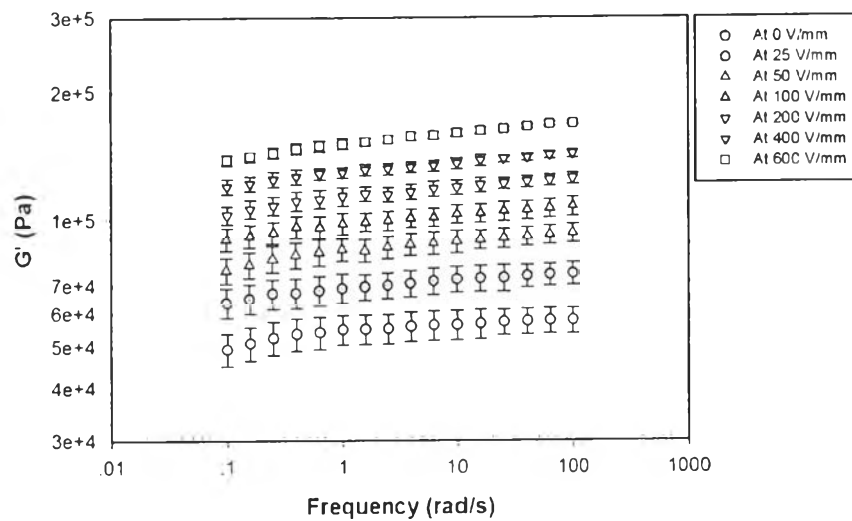


Figure L3 Frequency sweep test of silk fibroin/dedoped polycarbazole (0.01 %v/v of polycarbazole) hydrogel at strain 0.1 %, sample thickness 1.424 mm, temperature 300 K.

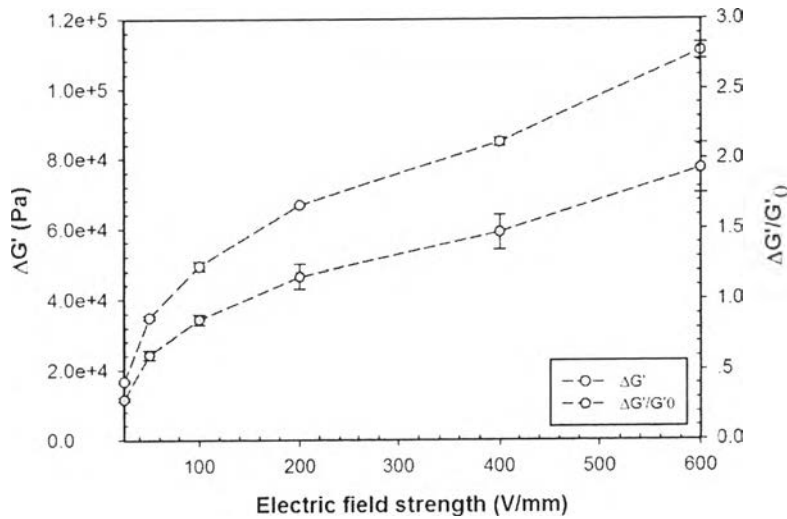


Figure L4 The storage modulus response ($\Delta G'$) and the storage modulus sensitivity ($\Delta G'/G'_0$) versus electric field strength of silk fibroin/dedoped polycarbazole (0.01 %v/v of polycarbazole) hydrogel at strain 0.1 %, frequency 100 rad/s, sample thickness 1.424 mm, temperature 300 K.

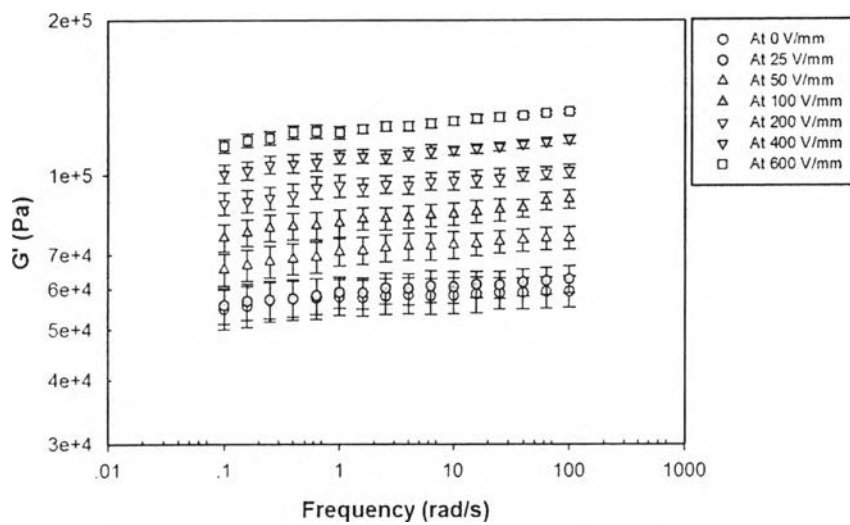


Figure L5 Frequency sweep test of silk fibroin/dedoped polycarbazole (0.1 %v/v of polycarbazole) hydrogel at strain 0.1 %, sample thickness 1.383 mm, temperature 300 K.

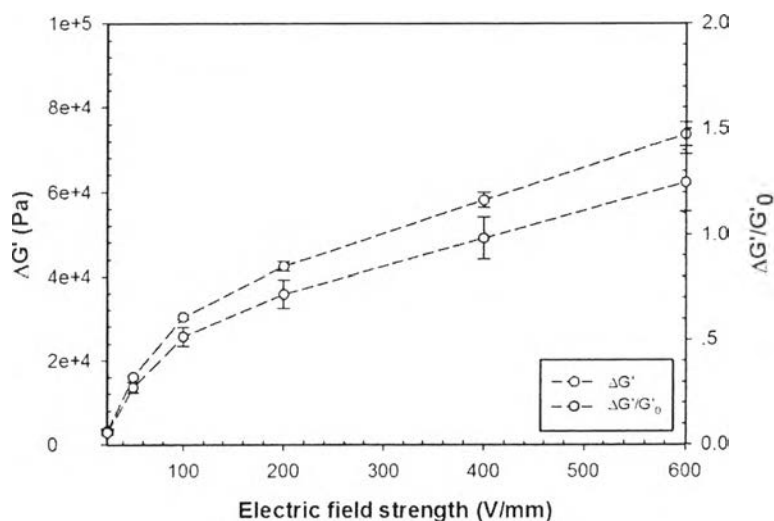


Figure L6 The storage modulus response ($\Delta G'$) and the storage modulus sensitivity ($\Delta G'/G'_0$) versus electric field strength of silk fibroin/dedoped polycarbazole (0.1 %v/v of polycarbazole) hydrogel at strain 0.1 %, frequency 100 rad/s, sample thickness 1.383 mm, temperature 300 K.

Table L1 The storage modulus responses and the storage modulus sensitivities of silk fibroin/dedoped polycarbazole (SF/De_PCZ) composite

Material	PCZ (%v/v)	Electric field strength (V/mm)	Frequency (rad/s)	Temperature (K)	Storage modulus response ($\Delta G'$) (Pa)	Initial storage modulus (G'_0) (Pa)	Storage modulus sensitivity ($\Delta G' / G'_0$)
SF/De_PCZ	0	600	100	300	2.42×10^5	4.12×10^4	5.87
SF/De_PCZ	0.001				1.37×10^5	4.71×10^4	2.90
SF/De_PCZ	0.01				1.11×10^5	5.77×10^4	1.92
SF/De_PCZ	0.1				7.36×10^4	5.94×10^4	1.24

Appendix M Dielectric Constant of Crosslinked Silk Fibroin Hydrogels, Silk Fibroin/Polycarbazole Hydrogels, and Silk Fibroin/Dedoped Polycarbazole Hydrogels

The dielectric constant values were measured by an LCR meter (HP, model 4284A) connected to the melt rheometer (Rheometric Scientific, ARES) with parallel plate fixture in diameter of 25 mm and the thickness of the samples of about 1 mm. The sample was sandwiched in between polyimide sheets. The top and bottom sides of parallel plate fixture were coated with a silver adhesive to improve electrical contact between specimens and the electrodes. The measurements were carried out at temperature of 300 K.

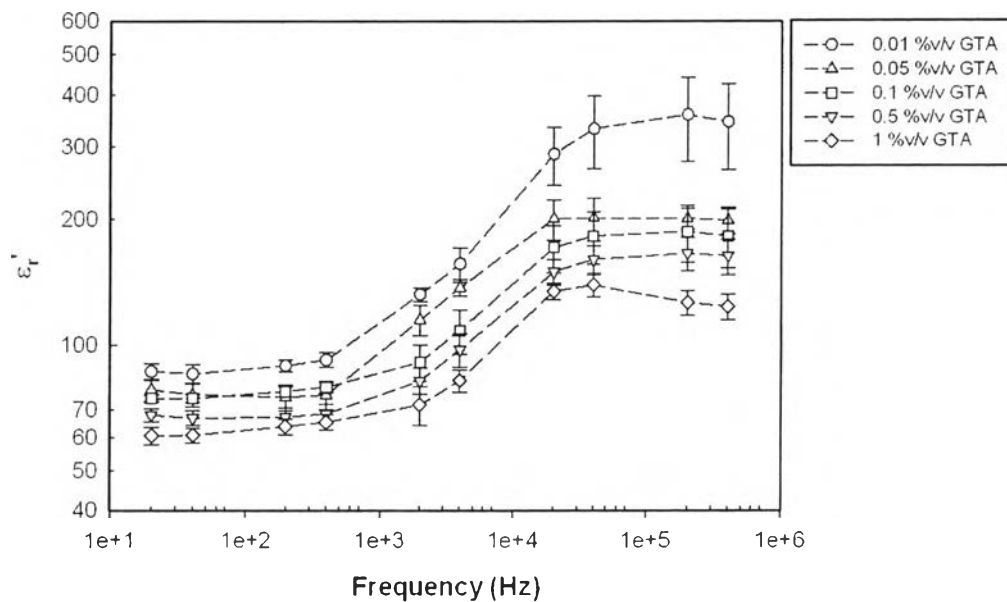


Figure M1 Relative dielectric constant (ϵ_r') versus frequency of crosslinked 4 %v/v silk fibroin solution with various amount of glutaraldehyde (GTA) at temperature of 300 K.

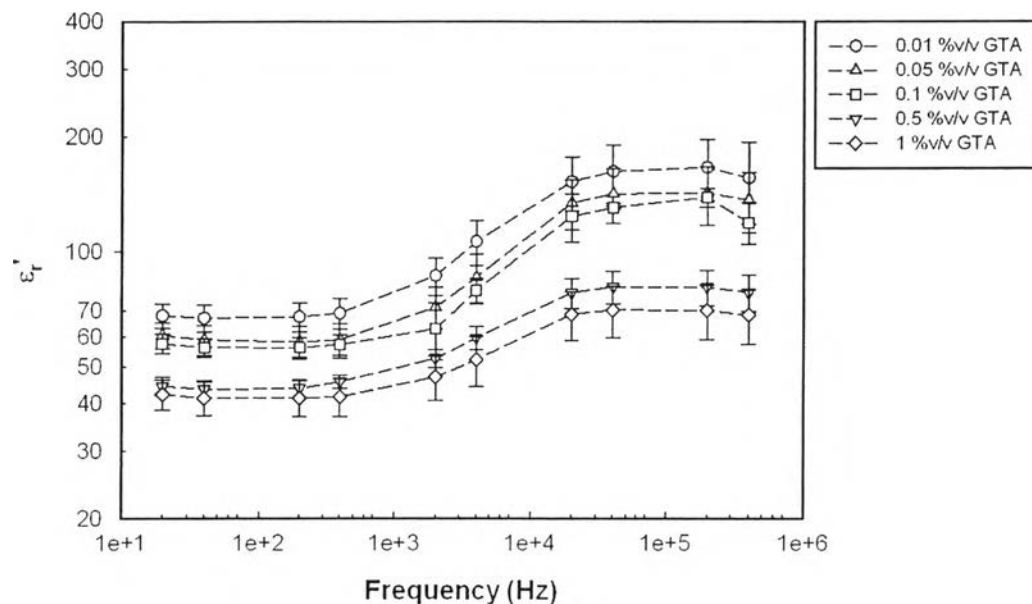


Figure M2 Relative dielectric constant (ϵ'_r) versus frequency of crosslinked 5 %v/v silk fibroin solution with various amount of glutaraldehyde (GTA) at temperature of 300 K.

Table M1 Comparison of the relative dielectric constant values of crosslinked silk fibroin (SF) hydrogels

Materials	Glutaraldehyde (%v/v)	Relative dielectric constant (ϵ'_r) at $\omega = 20$ Hz	Relative dielectric constant (ϵ'_r) at $\omega = 4.0 \times 10^5$ Hz
4 %v/v SF solution	0.01	86.42	344.33
	0.05	78.11	199.26
	0.1	74.43	182.31
	0.5	67.95	163.32
	1.0	60.64	123.66
5 %v/v SF solution	0.01	68.70	155.90
	0.05	60.42	136.65
	0.1	57.43	119.33
	0.5	44.46	78.28
	1.0	42.30	68.28

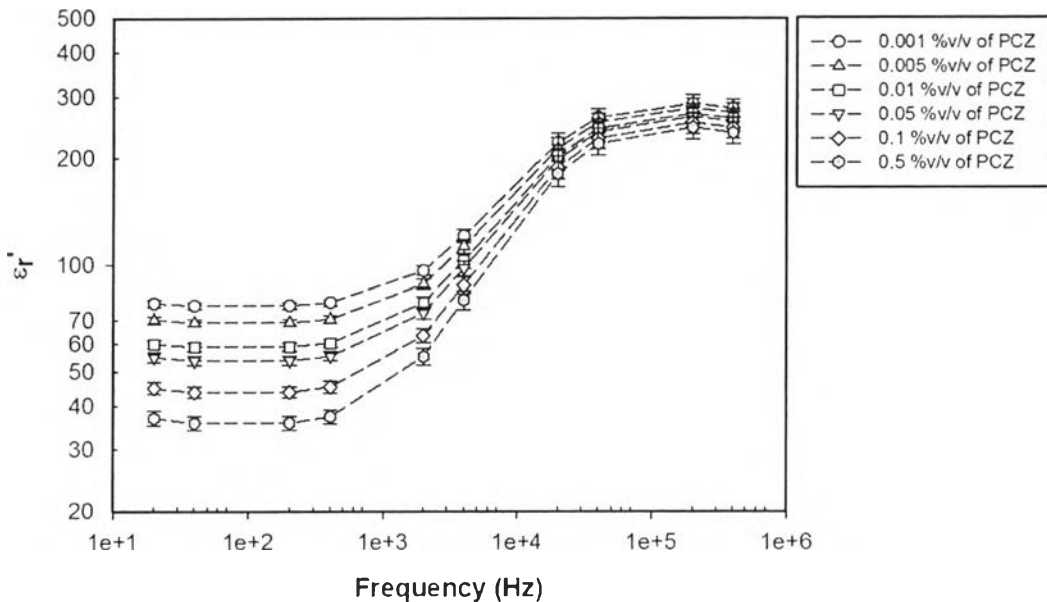


Figure M3 Relative dielectric constant (ϵ'_r) versus frequency of silk fibroin/polycarbazole (SF/PCZ) hydrogels with various polycarbazole (PCZ) concentration at temperature of 300 K.

Table M2 The relative dielectric constant values of silk fibroin/polycarbazole (SF/PCZ) hydrogels

Material	PCZ (%v/v)	Relative dielectric constant (ϵ'_r) at $\omega = 20$ Hz	Relative dielectric constant (ϵ'_r) at $\omega = 4.0 \times 10^5$ Hz
SF/PCZ	0.001	77.95	277.46
SF/PCZ	0.005	68.72	266.52
SF/PCZ	0.01	59.94	260.76
SF/PCZ	0.05	54.67	255.12
SF/PCZ	0.10	42.34	242.42
SF/PCZ	0.50	37.42	235.89

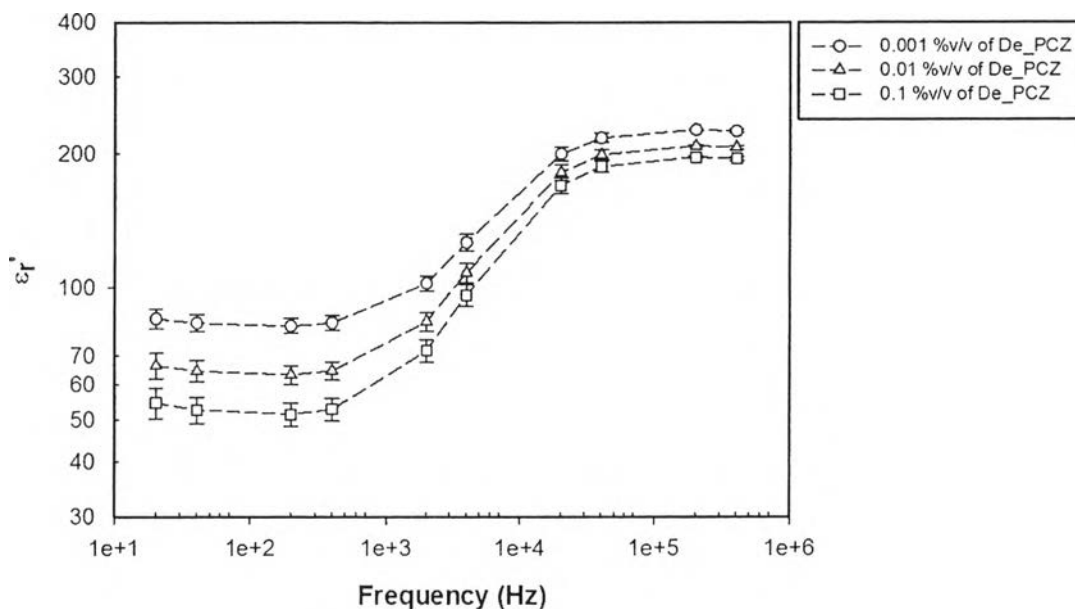


Figure M4 Relative dielectric constant (ϵ'_r) versus frequency of silk fibroin/de-doped polycarbazole (SF/De_PCZ) hydrogels with various dedoped polycarbazole (De_PCZ) concentration at temperature of 300 K.

Table M3 The relative dielectric constant values of silk fibroin/dedoped polycarbazole (SF/De_PCZ) hydrogels

Material	PCZ (%v/v)	Relative dielectric constant (ϵ'_r) at $\omega = 20$ Hz	Relative dielectric constant (ϵ'_r) at $\omega = 4.0 \times 10^5$ Hz
SF/De_PCZ	0.001	84.73	225.10
SF/De_PCZ	0.01	66.36	206.73
SF/De_PCZ	0.1	54.52	194.89

Appendix N Deflection responses of pure silk fibroin hydrogel and silk fibroin/polycarbazole (SF/PCZ) hydrogels

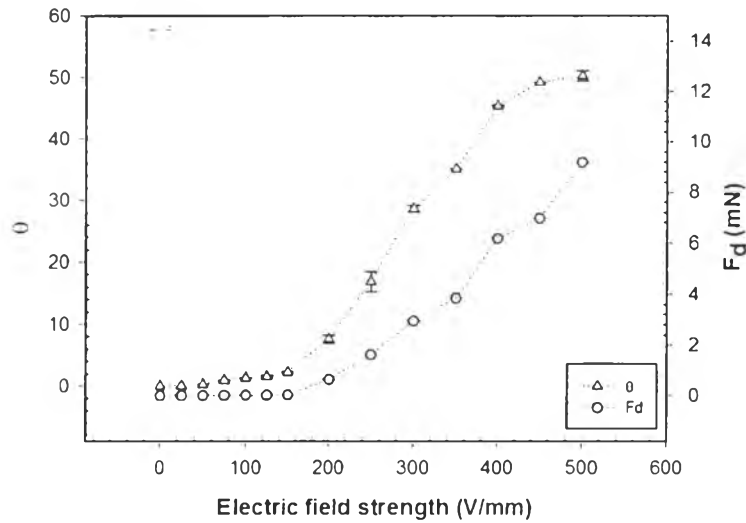


Figure N1 Deflection angle (θ) and dielectrophoresis force (F_d) versus electric field strength of pure silk fibroin hydrogel (sample width 3 mm, sample thickness 1.25 mm, sample weight 0.0855 g).

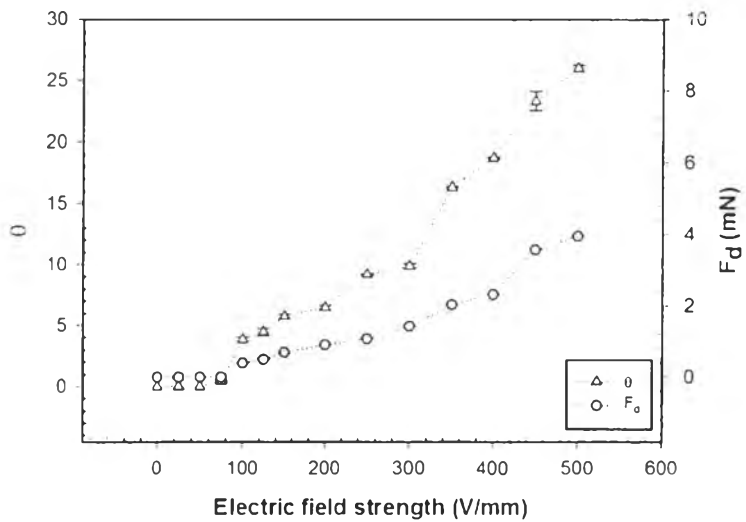


Figure N2 Deflection angle (θ) and dielectrophoresis force (F_d) versus electric field strength of SF/PCZ (0.001 %v/v of PCZ) hydrogel (sample width 3 mm, sample thickness 1.12 mm, and sample weight 0.0941 g).

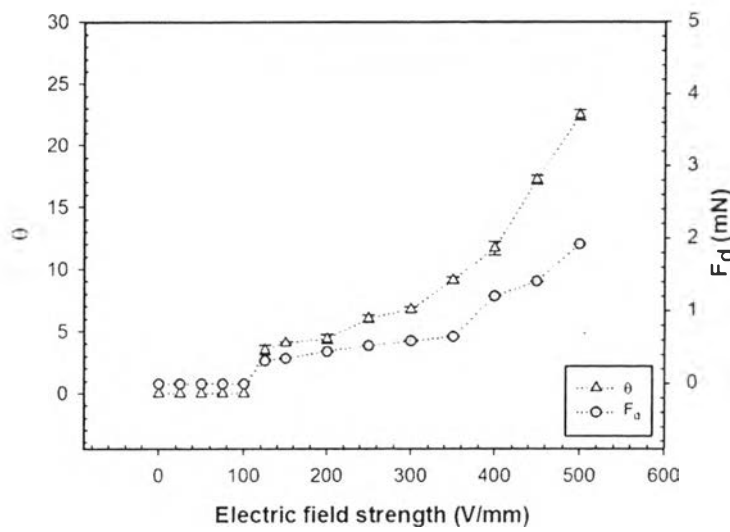


Figure N3 Deflection angle (θ) and dielectrophoresis force (F_d) versus electric field strength of SF/PCZ (0.005 %v/v of PCZ) hydrogel (sample width 3 mm, sample thickness 1.61 mm, and sample weight 0.1187 g).

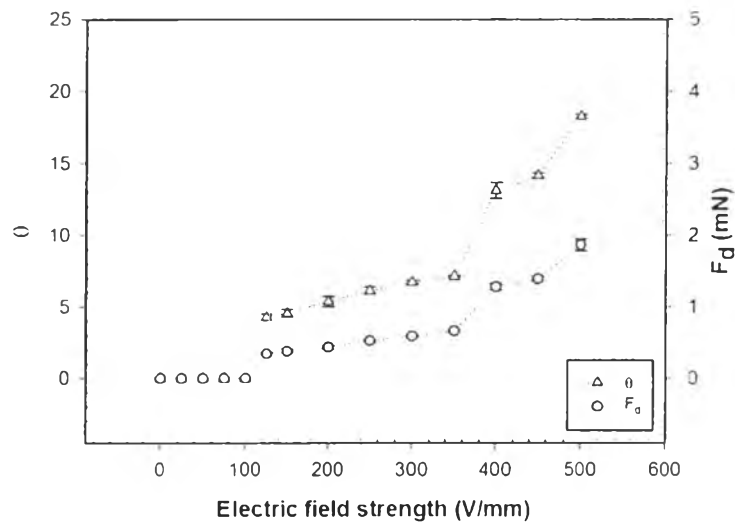


Figure N4 Deflection angle (θ) and dielectrophoresis force (F_d) versus electric field strength of SF/PCZ (0.01 %v/v of PCZ) hydrogel (sample width 3 mm, sample thickness 1.22 mm, and sample weight 0.0779 g).

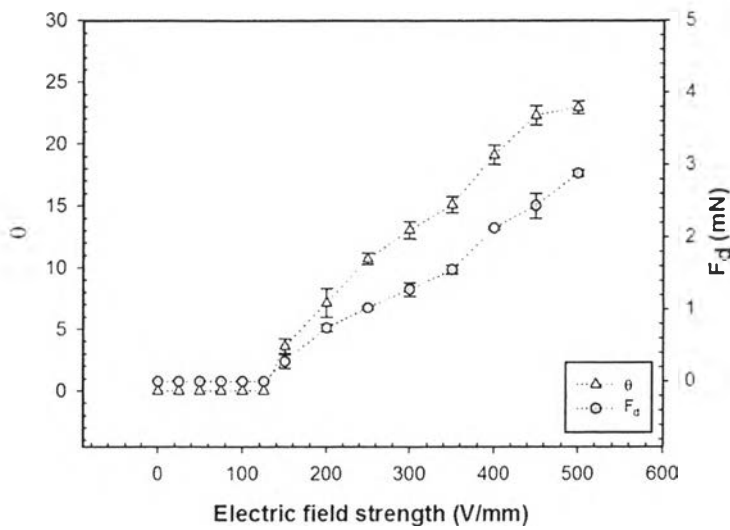


Figure N5 Deflection angle (θ) and dielectrophoresis force (F_d) versus electric field strength of SF/PCZ (0.05 %v/v of PCZ) hydrogel (sample width 3 mm, sample thickness 1.20 mm, and sample weight 0.0602 g).

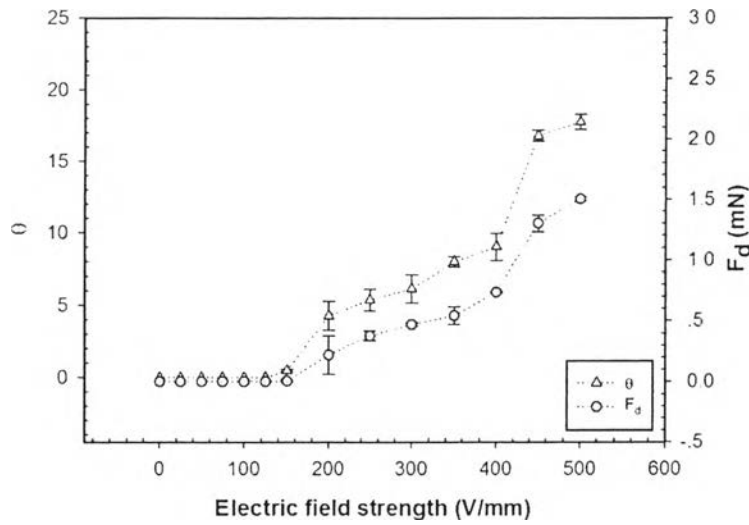


Figure N6 Deflection angle (θ) and dielectrophoresis force (F_d) versus electric field strength of SF/PCZ (0.1 %v/v of PCZ) hydrogel (sample width 3 mm, sample thickness 1.40 mm, and sample weight 0.1224 g).

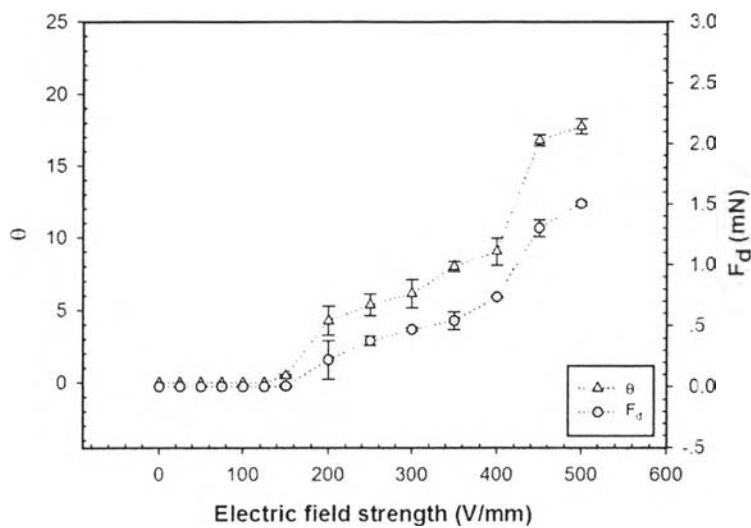


Figure N7 Deflection angle (θ) and dielectrophoresis force (F_d) versus electric field strength of SF/PCZ (0.5 %v/v of PCZ) hydrogel (sample width 3 mm, sample thickness 1.25 mm, and sample weight 0.1197 g).

Table N1 Deflection angles, deflection distances, and dielectrophoresis forces of silk fibroin/polycarbazole (SF/PCZ) composites at electric field strength of 500 V/mm.

Materials	PCZ (%v/v)	Deflection angle (θ) (°)	Deflection distance (mm)	Dielectrophoresis force (F_d) (mN)
SF/PCZ	0	50.78	8.00	9.19
SF/PCZ	0.001	26.17	5.11	2.32
SF/PCZ	0.005	23.54	4.53	3.95
SF/PCZ	0.01	22.15	4.11	1.67
SF/PCZ	0.05	18.17	2.79	1.93
SF/PCZ	0.1	23.31	4.44	2.92
SF/PCZ	0.5	18.18	3.70	1.51

CURRICULUM VITAE

Name: Ms. Thanida Srisawasdi

Date of Birth: October 2, 1987

Nationality: Thai

University Education:

2006–2010 Bachelor Degree of Science, Faculty of Science,
Chulalongkorn University, Bangkok, Thailand

Work Experience:

2010-2011	Position:	Research and development officer
	Company name:	Applied DB Industrial Co., Ltd.

Proceedings:

1. Srisawasdi, T.; Sirivat, A.; and Jamieson, A.M. (2013, April 23) Silk Fibroin/Polycarbazole Composite as Artificial Muscle. Proceedings of the 4th Research Symposium on Petrochemical and Materials Technology and the 19th PPC Symposium on Petroleum, Petrochemicals, and Polymers. Bangkok, Thailand.

Presentations:

1. Srisawasdi, T.; Sirivat, A.; and Jamieson, A.M. (2013, April 22) Development of Silk Fibroin/Polycarbazole Composite as Artificial Muscle. Paper Presented at the 1st Annual Symposium Conductive and Electroactive Polymer. Bangkok, Thailand.
2. Srisawasdi, T.; Sirivat, A.; and Jamieson, A.M. (2013, April 23) Silk Fibroin/Polycarbazole Composite as Artificial Muscle. Paper Presented at the 4th Research Symposium on Petrochemical and Materials Technology and the 19th PPC Symposium on Petroleum, Petrochemicals, and Polymers. Bangkok, Thailand.
3. Srisawasdi, T.; Sirivat, A.; and Jamieson, A.M. (2013, May 21-23) Silk Fibroin/Polycarbazole Composite as Artificial Muscle under Electric Field. Paper Presented at the 3rd International Symposium Frontiers in Polymer Science in Association with the Journal Polymer, Sitges, Spain.